FINAL REPORT FOR JUNE 1981 TO MAY 1982

ORBITER GLOBAL POSITIONING SYSTEM DESIGN AND KU-BAND PROBLEM INVESTIGATIONS EXHIBIT B - REVISION 1

(NASA-CR-171700) ORBITER GLOBAL POSITIONING SYSTEM DESIGN AND Ku-BAND PROBLEM INVESTIGATIONS, EXHIBIT B, REVISION 1 Final Report, Jun. 1981 - May 1982 (LinCom Corp., Los Angeles, Calif.) 90 p HC A05/MF A01 G3/04

N83-34929

Unclas
42163

PREPARED FOR

NASA LYNDON B. JOHNSON SPACE CENTER
HOUSTON, TX 77058

TECHNICAL MONITOR: WILLIAM TEASDALE

CONTRACT NO. NAS9-16097

TR-0783-0980

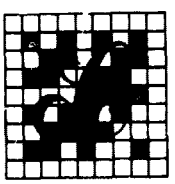

LinCom Corporation

P.O. BOX 15897, LOS ANGELES, CALIFORNIA 90015

LinCom

FINAL REPORT FOR JUNE 1981 TO MAY 1982

ORBITER GLOBAL POSITIONING SYSTEM DESIGN AND KU-BAND PROBLEM INVESTIGATIONS

EXHIBIT B - REVISION 1

PREPARED FOR

NASA LYNDON B. JOHNSON SPACE CENTER
HOUSTON, TX 77058

TECHNICAL MONITOR: WILLIAM TEASDALE

CONTRACT NO. NAS9-16097

PREPARED BY

W. C. LINDSEY

LINCOM CORPORATION
P.O. BOX 15897
LOS ANGELES, CA 90015

JULY 1983

TR-0783-0980

LinCom

TABLE OF CONTENTS

1. Introduction

This report serves to document the LinCom effort under Exhibit B of Contract NAS 9-16097 for the period June 1, 1981 through May 30, 1982. The purpose of Exhibit B is to support JSC in its study of the use of the GPS navigation system on the Space Shuttle Orbiter and in Ku-Band problem investigations. Additionally, under instruction from JSC a design study of some communication waveforms to be used on the Space Station was undertaken.

2. Effort Related to GPS

In support of the GPS study, LinCom was tasked to perform engineering support, primarily of an analytical nature, to assist NASA in making sound technical decisions regarding the design and operation of the Orbiter GPS Subsystem.

Part of LinCom's work in this area was an investigation of the hardware, the software, and the interface between them for a low dynamics, nonhostile environment, low-cost GPS receiver, the GPS Z-set. This study is documented in Attachment 1.

After the time the Z-set report was issued (September 10, 1982), LinCom's effort in the GPS area ceased on instructions from JSC. For this reason, no recommendations for additional areas of investigative effort are given.

3. Effort Related to Ku-Band System

3.1 Introduction

In support of the Orbiter Ku-band system problem investigation, LinCom was tasked to provide independent technical evaluation of the system performance evaluations.

3.2 Description of Effort

In partial completion of the work required here, LinCom attended the

monthly Ku-band program reviews at Hughes Aircraft Company Space and Communications Group in El Segundo, CA, and perceived many problem areas from the presentations and outside discussions. A preliminary assessment of the problems was provided on the spot or over the telephone to the JSC person concerned and the problems were later followed up.

3.3 Recommendations for Additional Areas of Investigative Effort

LinCom should continue to provide the same type of timely, comprehensive support to JSC that it has been providing.

4. Additional Effort

A design study was done for JSC on the waveform for the communication links between the Space Station and extra-vehicular activities/free-flyers. Frequency hopping was assumed to be used on the links in order to combat both noise and tone jamming. This effort is reported on in Attachments 2, 3, and 4.

LinCom

ATTACHMENT 1

GPS Z-SET HARDWARE/SOFTWARE INTERFACE

PREPARED FOR

NASA LYNDON B. JOHNSON SPACE CENTER
HOUSTON, TX 77058

TECHNICAL MONITOR: DR. JIM PAWLOWSKI

CONTRACT NO. NAS9-16097

PREPARED BY

ANIL V. KANTAK

LINCOM CORPORATION
P.O. BOX 15897
LOS ANGELES, CA 90015

SEPTEMBER 10, 1981

TR-0783-1180

LinCom

TABLE OF CONTENTS

1. Introduction

This report investigates the hardware, the software and the interface between them for a low dynamics, nonhostile environment, low cost GPS receiver (GPS Z-set). The set is basically a three dimensional geodetic and waypoint navigator with GPS time, ground speed and ground track as possible outputs in addition to the usual GPS receiver set outputs. In what follows, each functional module comprising the GPS set is described in brief, enumerating its functional inputs and outputs, leading to the interface between hardware and software of the set.

2. GPS Measurement Concept

The basic steps in GPS measurement concepts are described in the following steps:

1. Satellites radiate time tagged signals at L-band.
2. Multiple monitor stations observe the radiated signals.
3. Master station computed orbits and clock offsets.
4. Upload stations place data in each satellite.
5. Satellites broadcast data as modulation on signals.
6. User receiver observes signal arrival time.
7. Making corrections and knowing satellite position user obtains own position and clock offset.

2.1 Range Measurement

There are two types of range measurements necessary in any GPS receiver set. They are:

1. Pseudo Range = Satellite clock error + equipment delay + free space + ionospheric delay + atmospheric delay + user equipment delay + user clock errors.
2. Delta Range = A measurement, over a known interval of time,

of the change in phase of the L-band carrier relative to a carrier synchronized from user's oscillator.

3. Receiver Partitioning

In what follows next, we will divide the receiver set into two partitions, (a) receiver software subsystems and (b) receiver hardware subsystems.

The receiver set can be divided into several separate functional modules each module having a set of inputs and outputs. Figure 1 depicts the functional modules of the set. In what follows, each of these modules will be described in brief. Inputs and outputs for each module will be defined, consequently leading to the interface definition between the software and hardware components of the system. The functional blocks of the set are:

1. Antenna, preamplifier module.
2. RF/IF module.
3. Phase lock module.
4. Synthesizer module.
5. Reference oscillator module.
6. Coder/user time clock module.
7. Baseband module.
8. I/O module.
9. CPU module.
10. ROM module.
11. Carrier and display unit modules.

Figure 1 shows the signal flow direction between modules of the receiver set. From the functional block diagram one can see that the

SET Z FUNCTIONAL MODULES

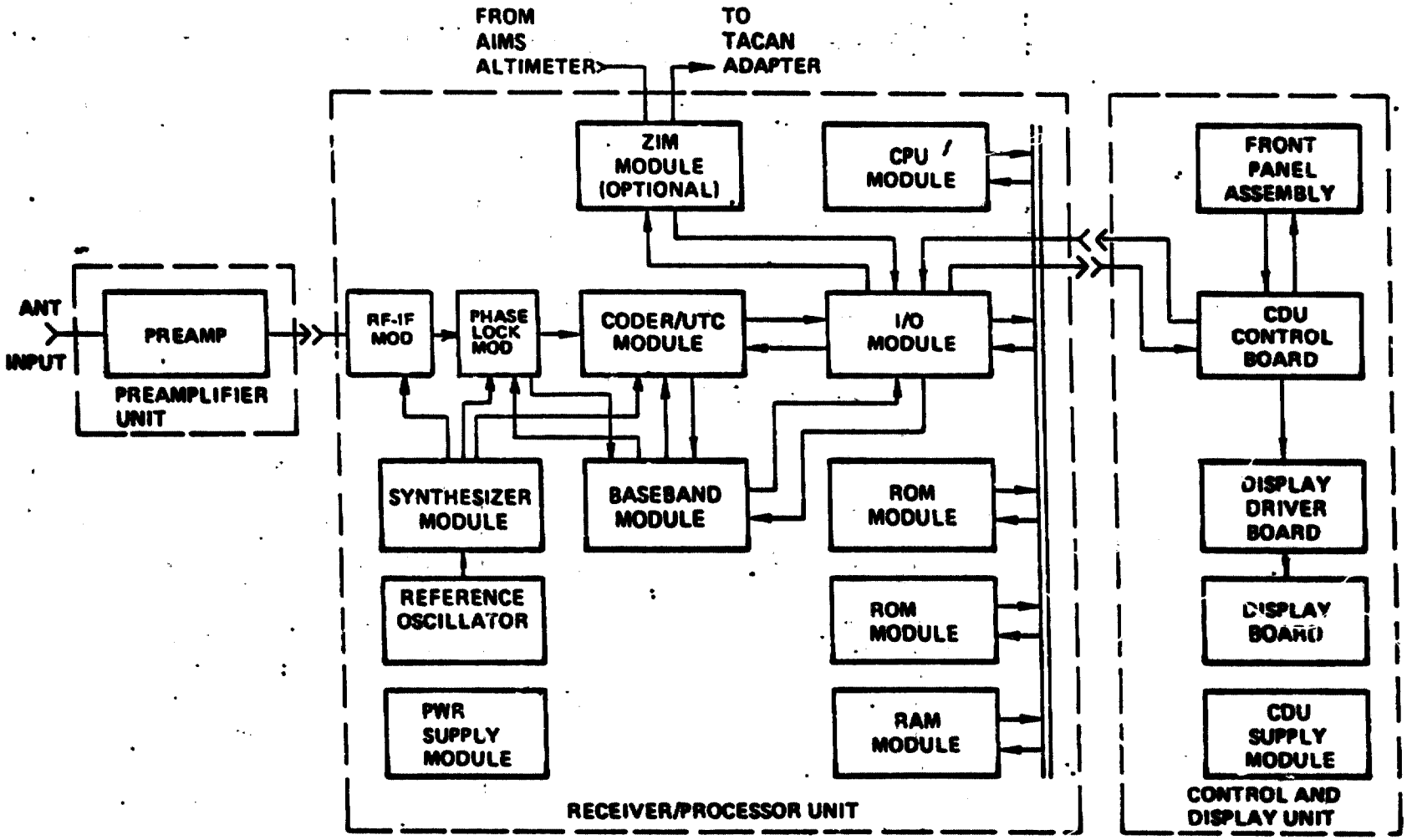

GENERAL DYNAMICS
Electronics Division

Figure 1 .

system can be partitioned into software and hardware subsystems for a better understanding of the operation of the set. This partitioning is shown in Figure 2. In what follows, we will describe the inputs and outputs of each functional module of the receiver/processor unit shown in Figure 1. Throughout this report F = 5.115 MHz.

3.1 RF-IF Module

The main purpose of this module is to accept the L-band signal from the antenna/preamplifier module and condition it (down convert) for the use of the subsequent modules. Figure 3 shows the RF-IF module block diagram.

RF-IF Module Inputs:

1. 308F, L-band signal from the antenna-preamplifier assembly.
2. Synthesizer inputs 68F, 29 1/2 F, 6F, 5F for the down convert operation.
3. Clock input from the user time clock.
4. Code input from the coder module to correlate with the incoming signal.
5. Command from central processing unit to switch to L_1 or L_2 frequency.
6. Input from the AGC circuit to the filter to maintain the signal level.

RF-IF Module Outputs:

1. 1 1/2 F frequency IF signal to the baseband module.
2. AFI output for determination of the signal quality.

3.2 Synthesizer

The main purpose of synthesizer is to produce various frequencies necessary for purposes of down converting, phase locking and code

SYSTEM PARTITIONING

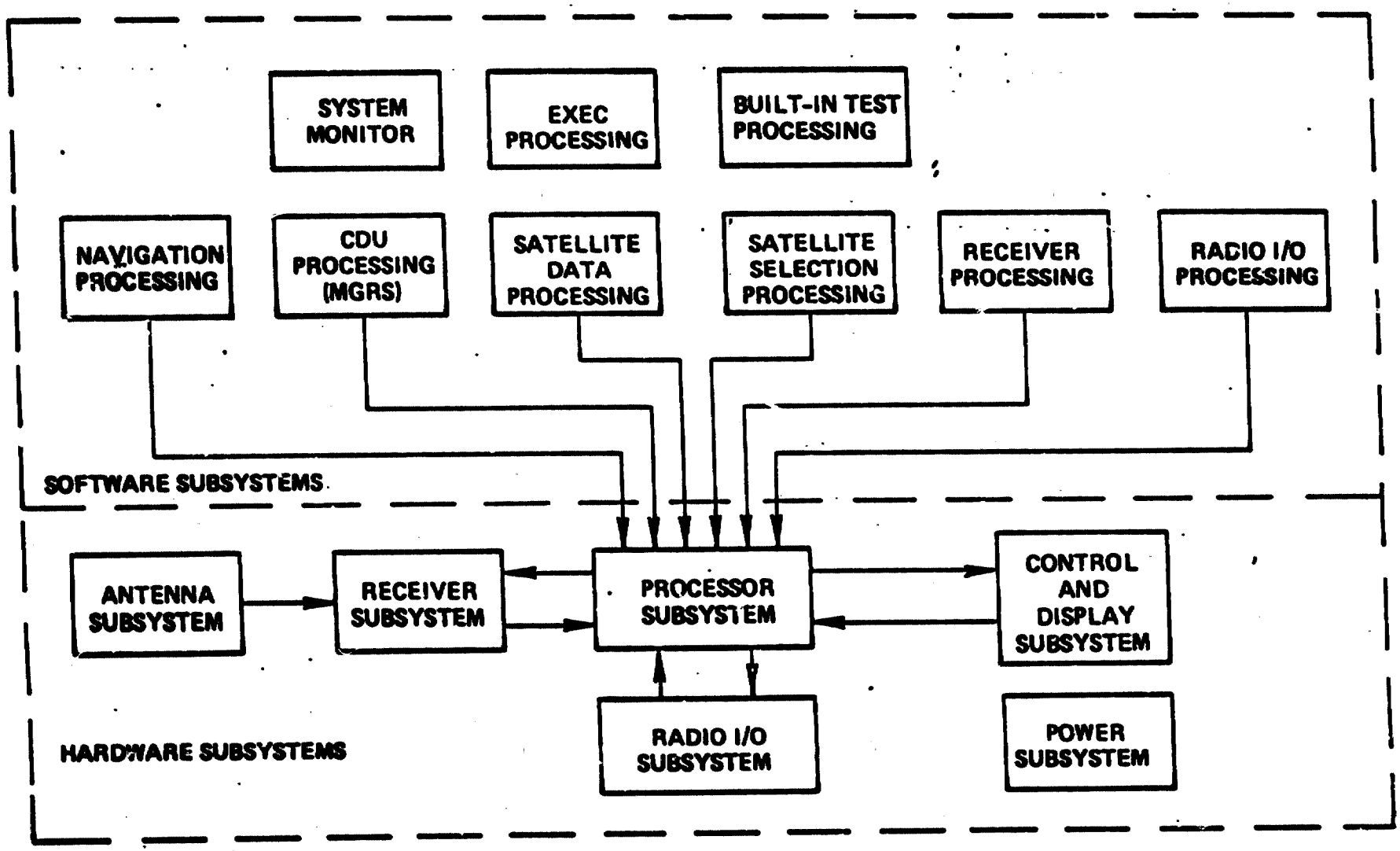

Figure 2.

GENERAL DYNAMICS
Electronics Division

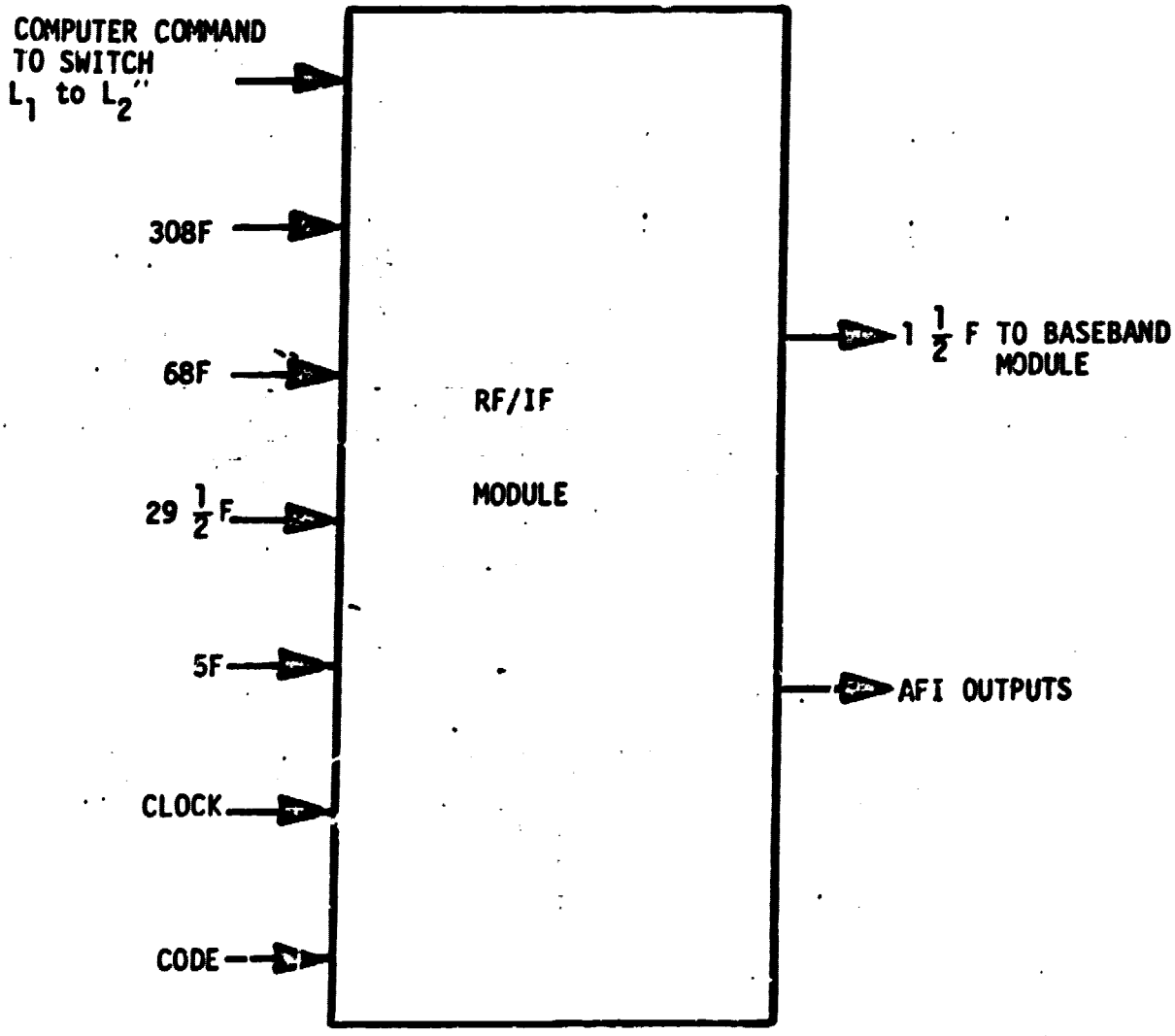

Figure 3. Inputs/Outputs of RF/IF Module.

generation, etc.

Synthesizer Inputs:

1. F from the VCO.
2. 1 1/2 F from the user time clock.
3. F/154 from the baseband module.
4. 120F.

Synthesizer Outputs:

1. 5F, 68F, 29 1/2 F to be used by RF/IF module for generating the baseband signal.
2. 6F and $2F_{CT}$ to user time clock.
3. $2F_{CT}$ to the coder module.

Combining the inputs and outputs described above we get the block diagram of the synthesizer as shown in Figure 4.

3.3 Phase Lock Module (PLM)

The main purpose of the phase lock module is to provide clock to baseband and coder modules.

Phase Lock Module Inputs:

1. 1 1/2 F IF signal.
2. 1 1/2 F signal necessary to split incoming IF into inphase and quadrature (I&Q) components.
3. The F and F/154 necessary to generate the coder input.

Phase Lock Module Outputs:

1. F_{VCO} output transmitted to baseband module for integrate and dump operation.
2. I&Q components of the signal to obtain the AGC, etc.
3. The 2F+D signal to coder to produce the time and coarse data range measurements.

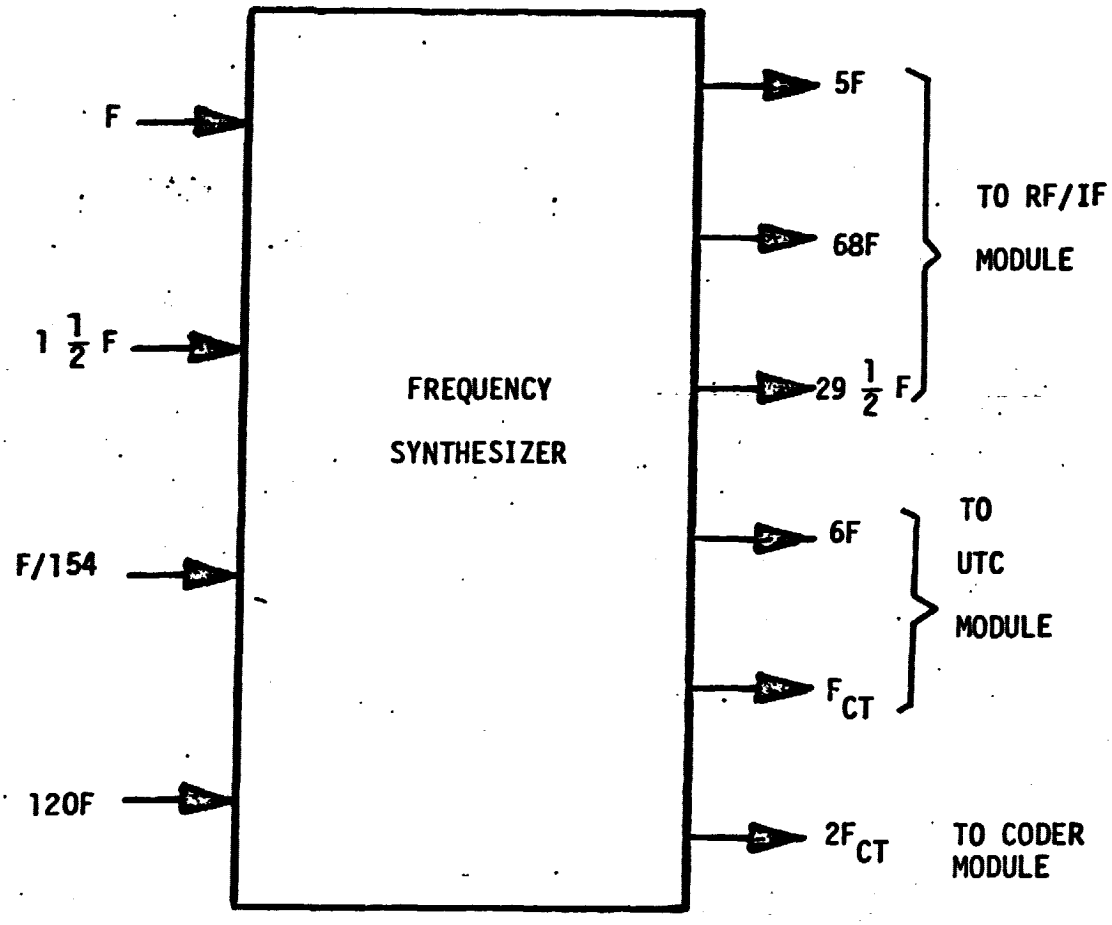

Figure 4. Inputs/Outputs of Frequency Synthesizer.

4. 2 1/2 F and F/10 + D outputs to be used in the baseband module.

Figure 5 depicts the phase lock module in block diagram from giving all the inputs and outputs.

3.4 Baseband Module

Baseband module is the heart of receiver. It detects the signal, tracks, demodulates and generates the AGC and the code loop error. Figure 6 describes the baseband analog design in block diagram form. We will divide the baseband module in four modules which are:

1. Costas loop, lock detector, VCO prepositioning and data detector.
2. AFC detector.
3. AGC detector and signal present detector.
4. Code loop error detector.

3.5 Costas Loop/Lock Detector/Preposition

Figure 7 shows Costas loop with the lock detector and VCO prepositioning circuit. This loop performs the locking to the incoming IF signal frequency, detects the lock and sends the lock achieved flag to the computer, it also detects the data for the subsequent operations on it like the bit synch. Finally, the loop also allows for prepositioning of VCO necessary for initial lock.

Costas Loop Configuration Inputs:

1. I and Q components from the PLM.
2. The input from AGC to the filter.
3. VCO prepositioning command from the computer.
4. 1/2 chip step to the pulse generator.
5. 1 msec and 20 msec clock from A/A coder.
6. 1/20 msec select from the computer.

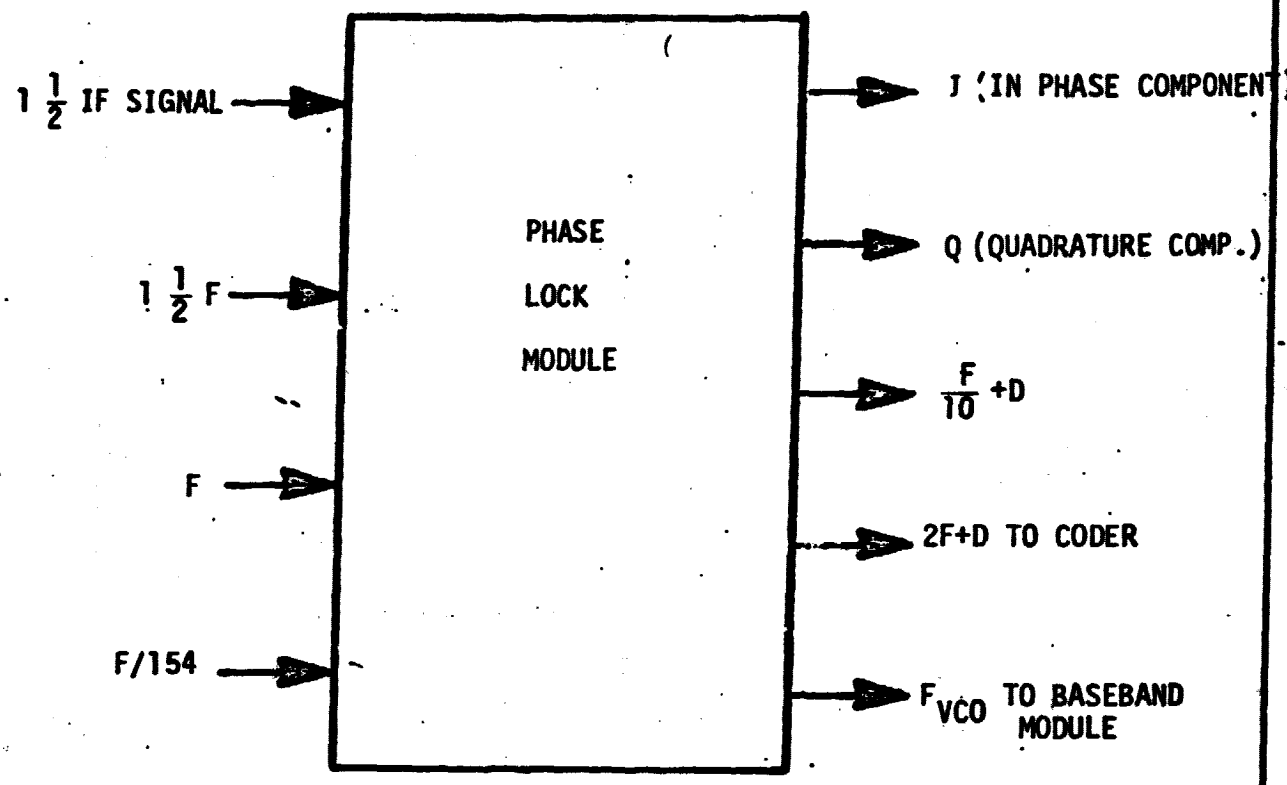

Figure 5. Inputs/Outputs of the Receiver Phase Lock Module.

BASEBAND ANALOG DESIGN

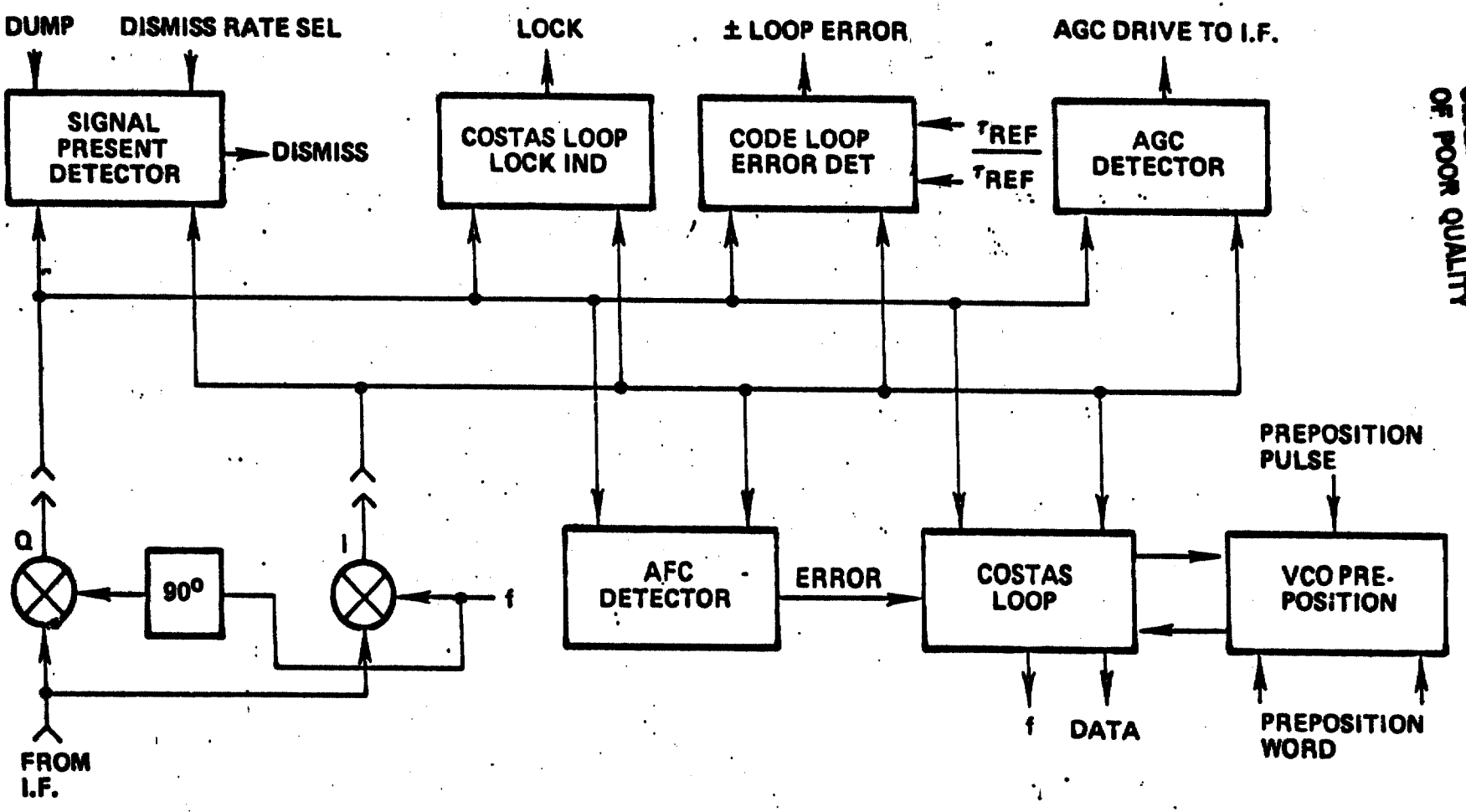

Figure 6.

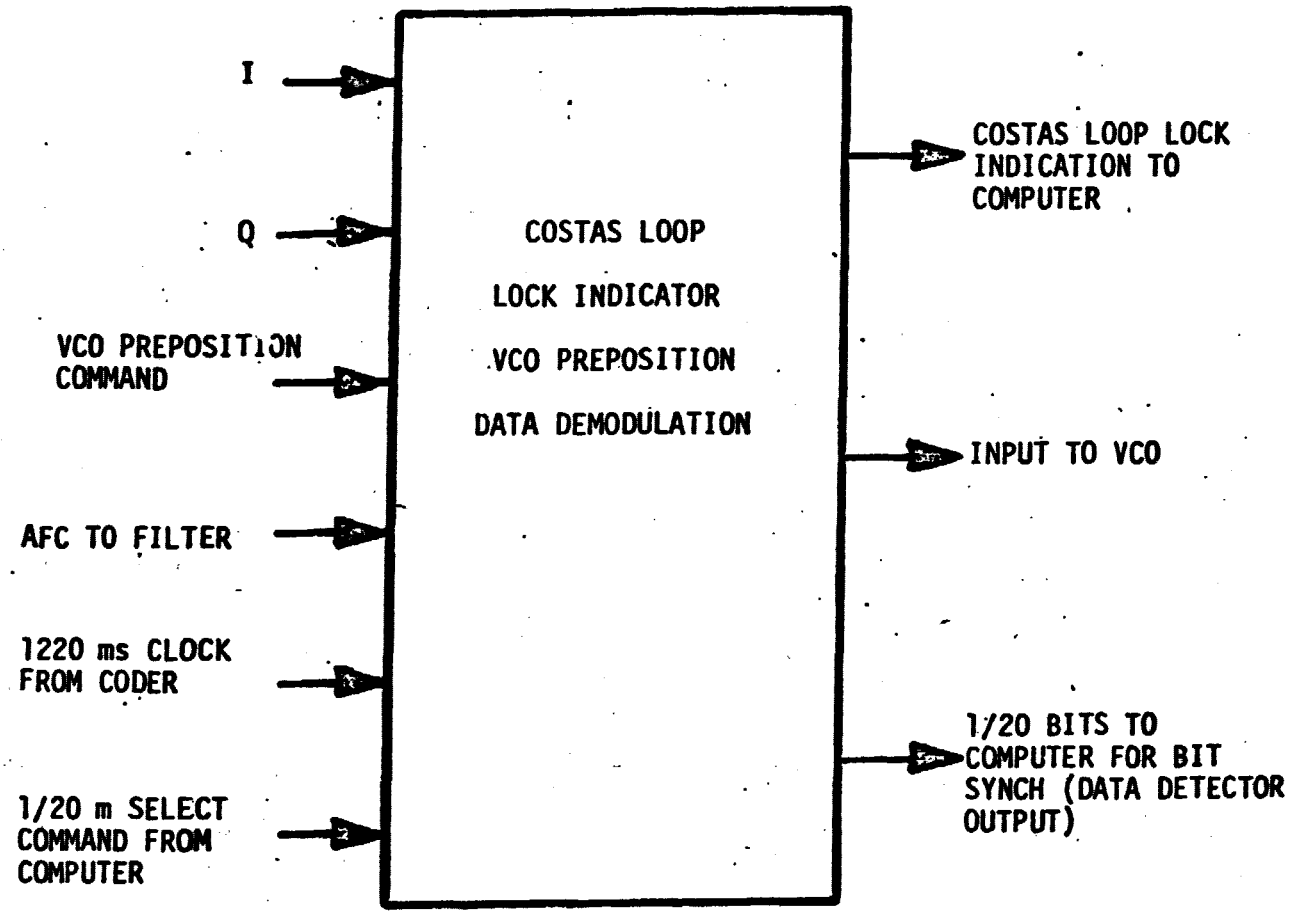

Figure 7. Inputs/Outputs of the Receiver Costas Loop Module.

Costas Loop Configuration Outputs:

1. Costas loop lock status to the computer.
2. Signal to the VCO.
3. 1/20 of bits to the computer for bit synch (data detector output).

3.6 AFC Detector

This loop accepts the inphase and quadrature components of signal and computes for AFC signal necessary for the Costas loop filter. Fig. 8 shows this loop.

3.7 Code Loop Error Detector and Phasing Control

The main purpose of this loop is to detect the code loop error and use this error to set the frequency of code clock to the right frequency.

Code Loop Error Detector Inputs:

1. I and Q components of the signal.
2. t reference.

Code Loop Error Detector Outputs:

1. Code phase error control.
2. Code clock to the doppler scaling circuit.

Figure 9 shows the code loop with the inputs and outputs in a block diagram form.

3.8 AGC and Sequential Detector

As the name suggests, this circuit is necessary for detecting if the signal is present and maintaining the signal level. Fig. 10 shows the AGC/sequential detector in a block diagram form.

Inputs/Outputs to AGC/Sequential Detector:

1. I&Q components of the incoming signal.

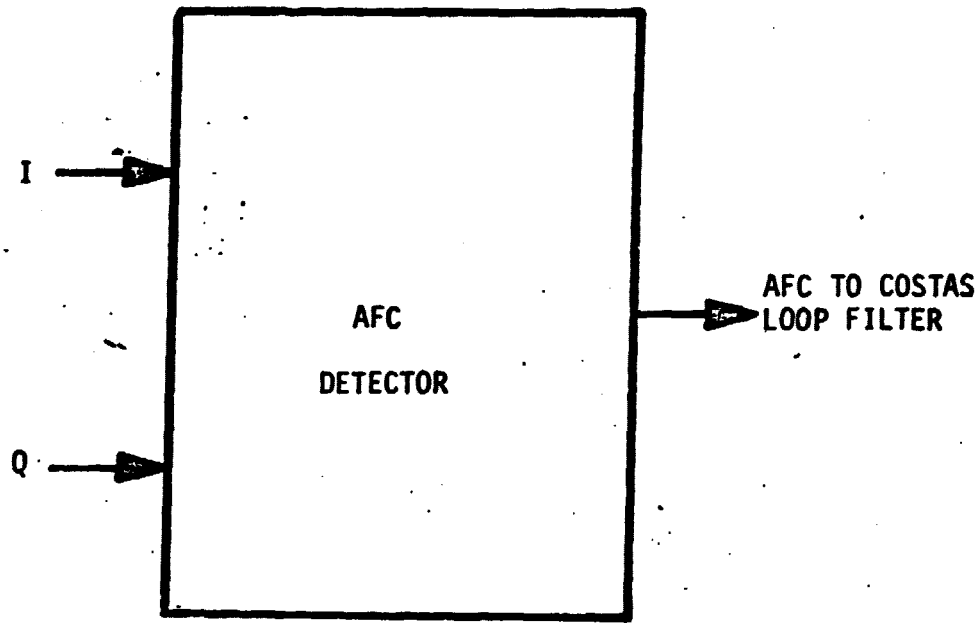

Figure 8. Inputs/Outputs of AFC Detector.

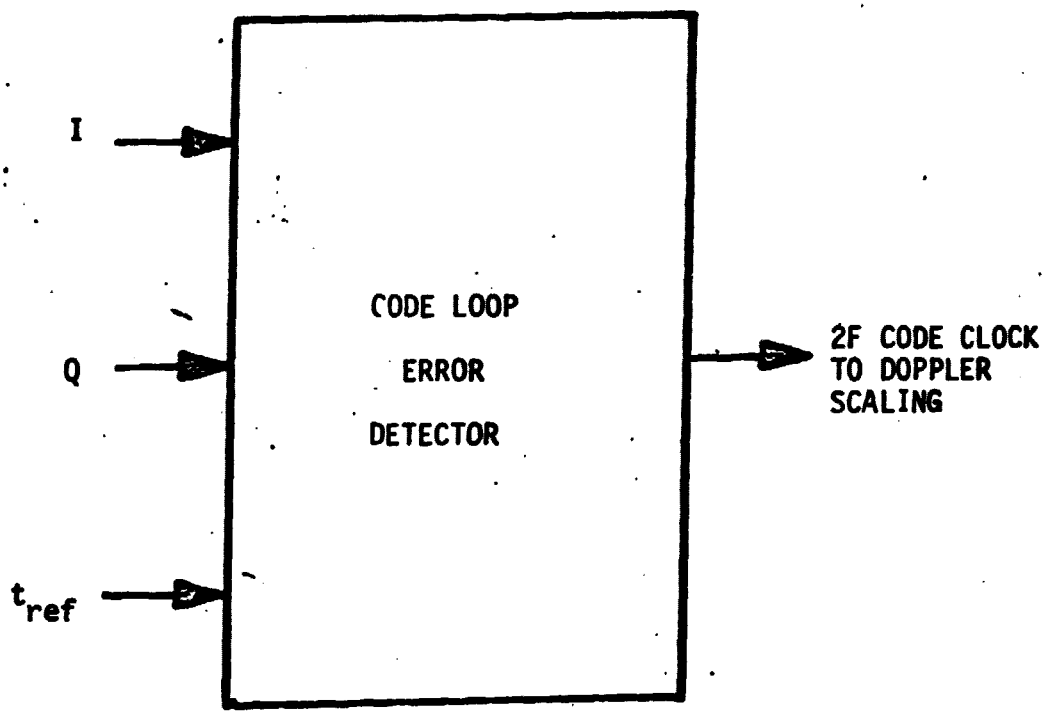

Figure 9. Inputs/Outputs of Receiver Set Code Loop Error Detector.

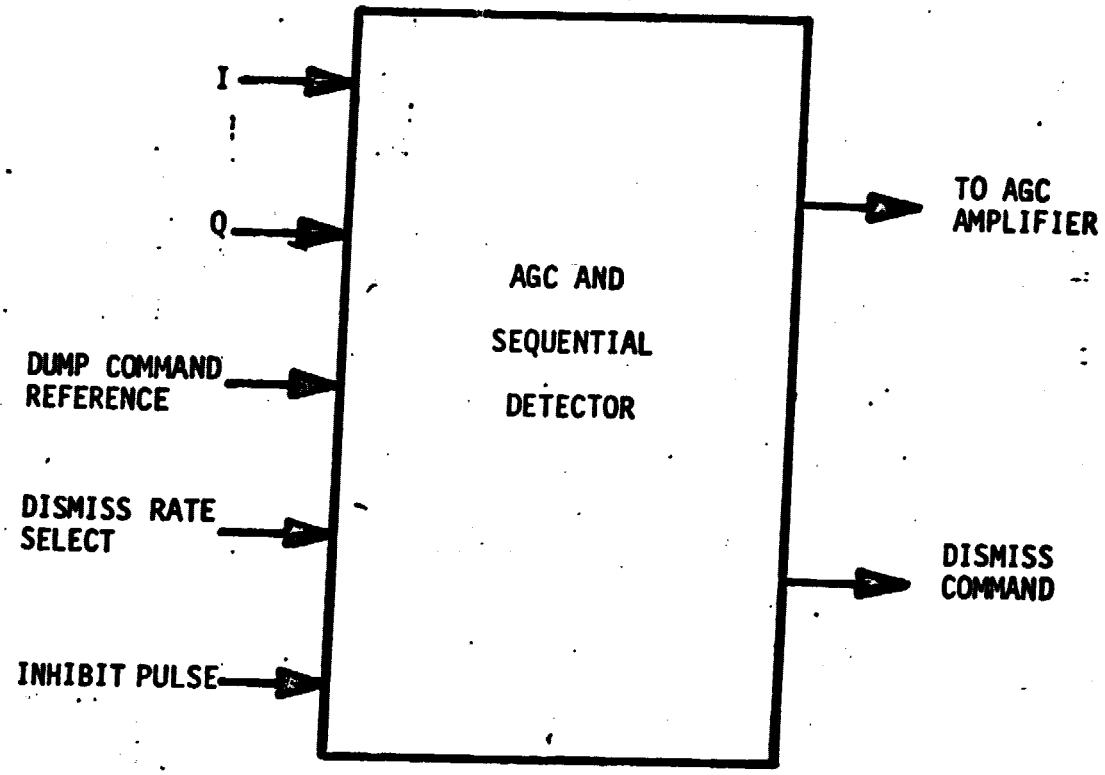

Figure 10. Inputs/Outputs of the AGC/Sequential Detector Module.

2. Start/inhibit input from computer.

3. Dismiss rate select.

4. Dump command output of control logic.

3.9 C/A Coder and Word Buffer

The clear acquisition coder basically produces the C/A code which is used for correlation with the receiver IF signal, in the baseband module (see Figure 11).

C/A Coder Input:

1. IF error signal from code loop error detector.

2. Bit clock phase command from computer.

C/A Coder Outputs:

1. C/A code.

2. 20 msec bit clock/intercept.

3. Coarse range epoch.

4. Bit clock word-buffer output to computer.

5. CT word buffer output to computer.

3.10 User Time Clock Module (UTC)

User time clock generates the clocking for various synchronization processes in the receiver circuit set. Figure 12 describes the inputs and outputs of user time module.

UTC Inputs:

1. 6F reference.

2. Coarse range, time and delta range epochs.

UTC Outputs:

1. 0.1 second UT interrupt.

2. UT word to computer.

3. CFDR (Coarse/Fire/Delta Range) to computer.

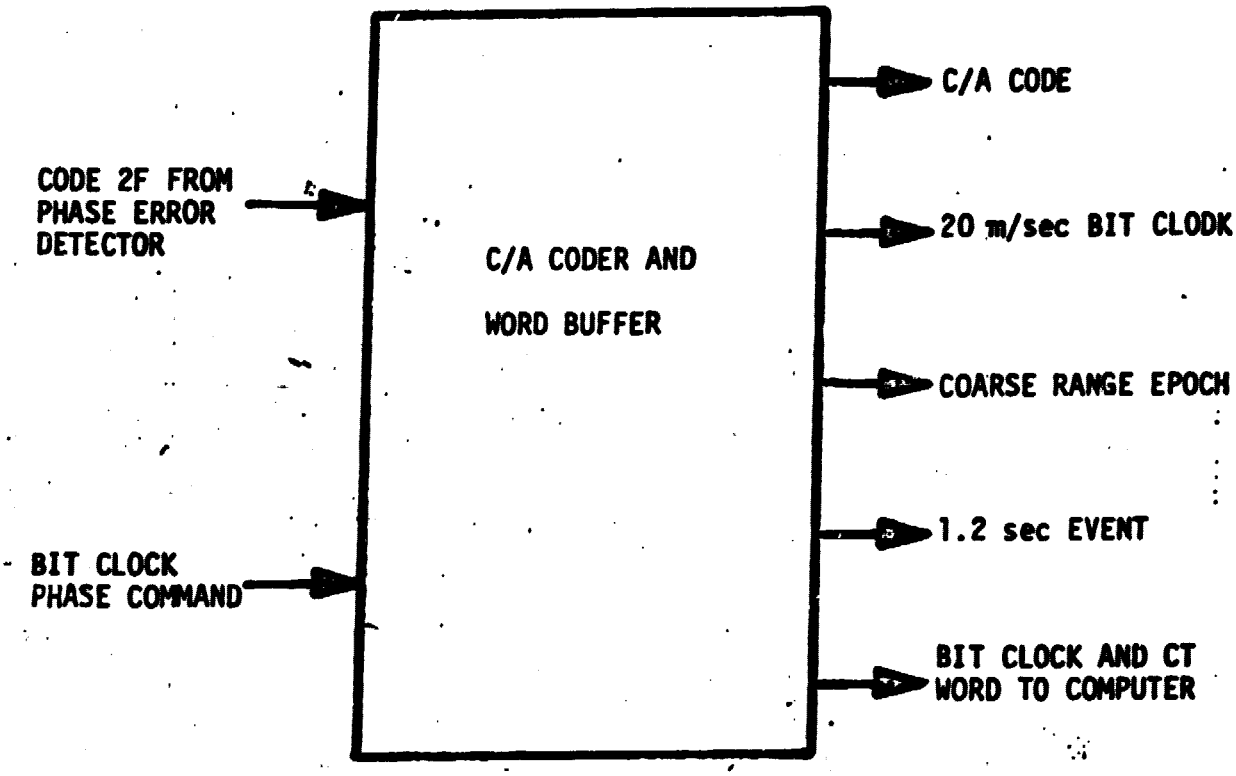

Figure 11. Inputs/Outputs of Receiver Set C/A Coder Module.

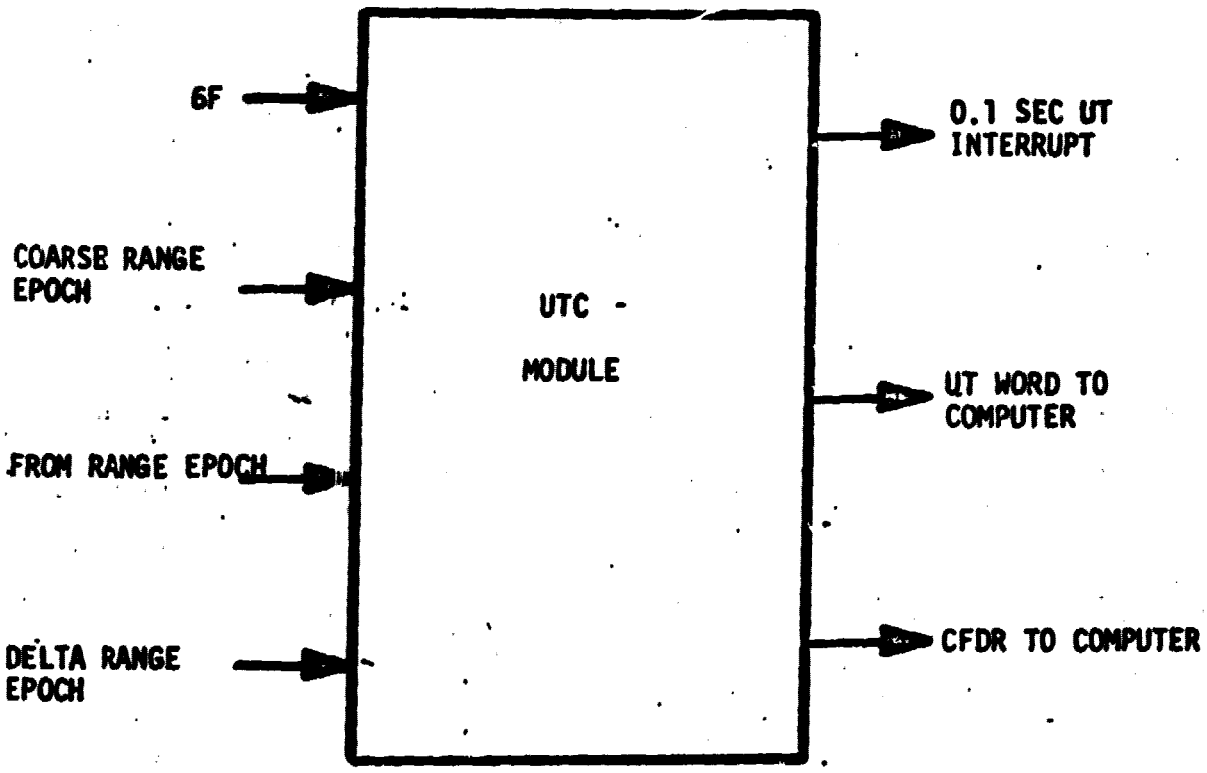

Figure 12. Inputs/Outputs of User Time Clock Module.

4. Software Subsystems

There are four basic parts in the software processing of the GPS receiver set. These are:

1. Navigation processing.
2. Satellite data processing.
3. Receiver processing.
4. Control display unit processing.

Each processing controls the hardware processing or uses the hardware outputs to compute the necessary parameters and in turn the executive processing controls the software processors.

Following pages describe the software processing enumerated above in brief, leading to the interface between the software and hardware systems.

4.1 Navigation Processing

It is a time division multiplexed processing of code, frequency and data obtained from each of the four satellite signals. The sequential measurement processng epochs are either 1.2 seconds or 1.8 seconds in duration. The main purpose of the navigation processor is to generate the necessary navigation prarmeters. It also generates the inputs for the satellite acquisition processing and the control display processor.

Functions:

1. Navigation processor does the estimation of navigation set position, velocity, clock bias, clock bias rate from GPS pseudorange and delta pseudorange measurement inputs from the coder loop. It also computes the acceleration of the set along with the altitude bias measurement. These computations are performed with 8 state Kalman filters.

2. Prediction of pseudorange and pseudorange rate at next sequential measurement epoch to preposition the code and frequency for satellite acquisition. The position and velocity is extrapolated to the time of next satellite to be processed in the sequence. This extrapolated position is combined with the clock bias to yield an estimate of the pseudorange and the extrapolated velocity is combined with the clock bias to generate the pseudorange rate estimate. The extrapolated pseudorange is converted to code chips and used to preposition the code state of the receiver. The extrapolated pseudorange rate is converted to a frequency offset and then used to preposition the frequency of the receiver.
3. Navigation processor converts the estimated position of the set to latitude, altitude and longitude. The estimated velocity is converted to ground speed and ground track.

Figure 13a describes the entire navigation processing overview showing the sequence in which the software routines are executed. Figure 13b shows the simple block diagram of inputs and outputs of the navigation processor.

4.2 Data Processor

The main prupose of the data processor is to collect the space vehicle ephemeris data used for accurate navigation and this data remains valid for 1.5 hours. The second purpose is the collection of almanac data which is useful to acquire new satellites, provide less accurate navigation and aid in satellite selection process. This data is valid up to one week.

The inputs of this processor are the bit value, the bit number, word number and space vehicle number. The processing determines if

NAVIGATION PROCESSING OVERVIEW FLOW

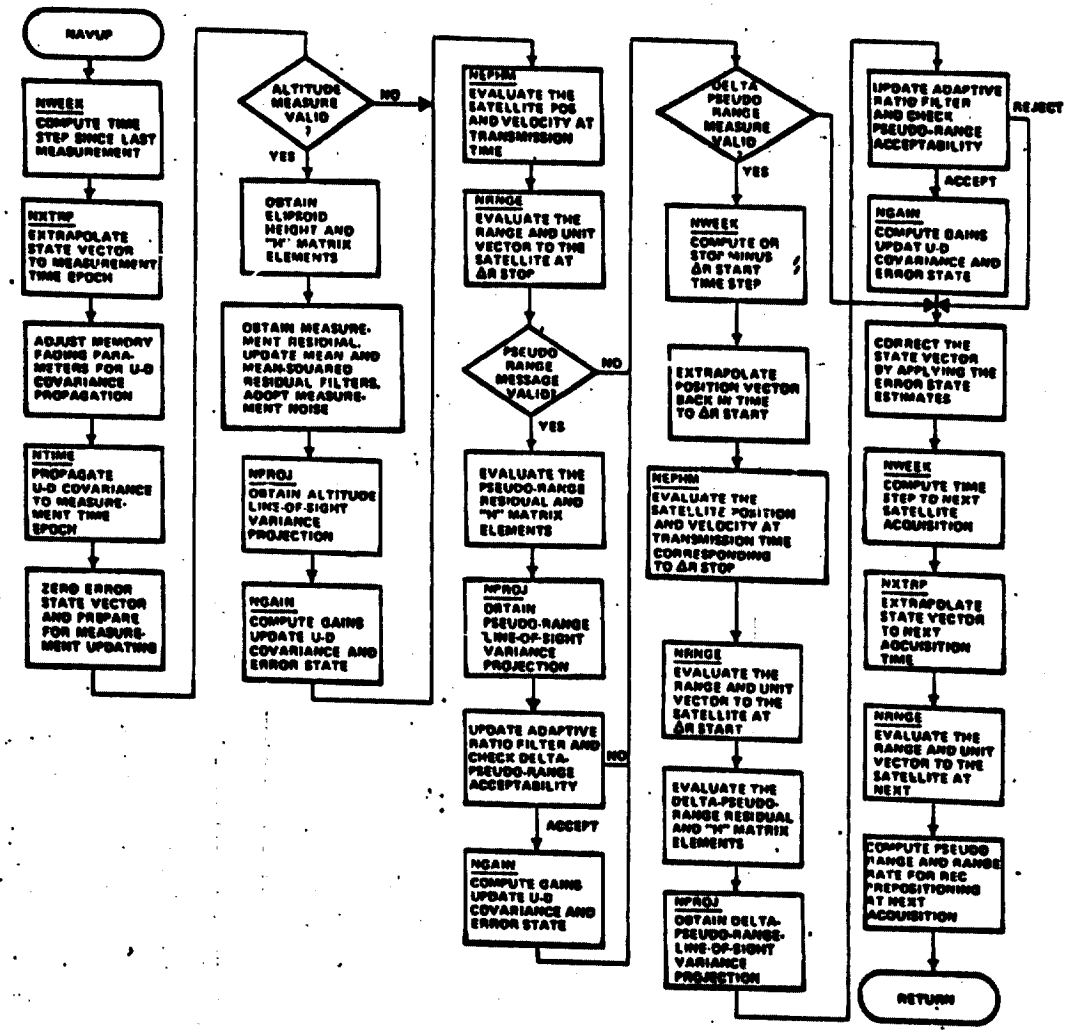

Figure 13a.

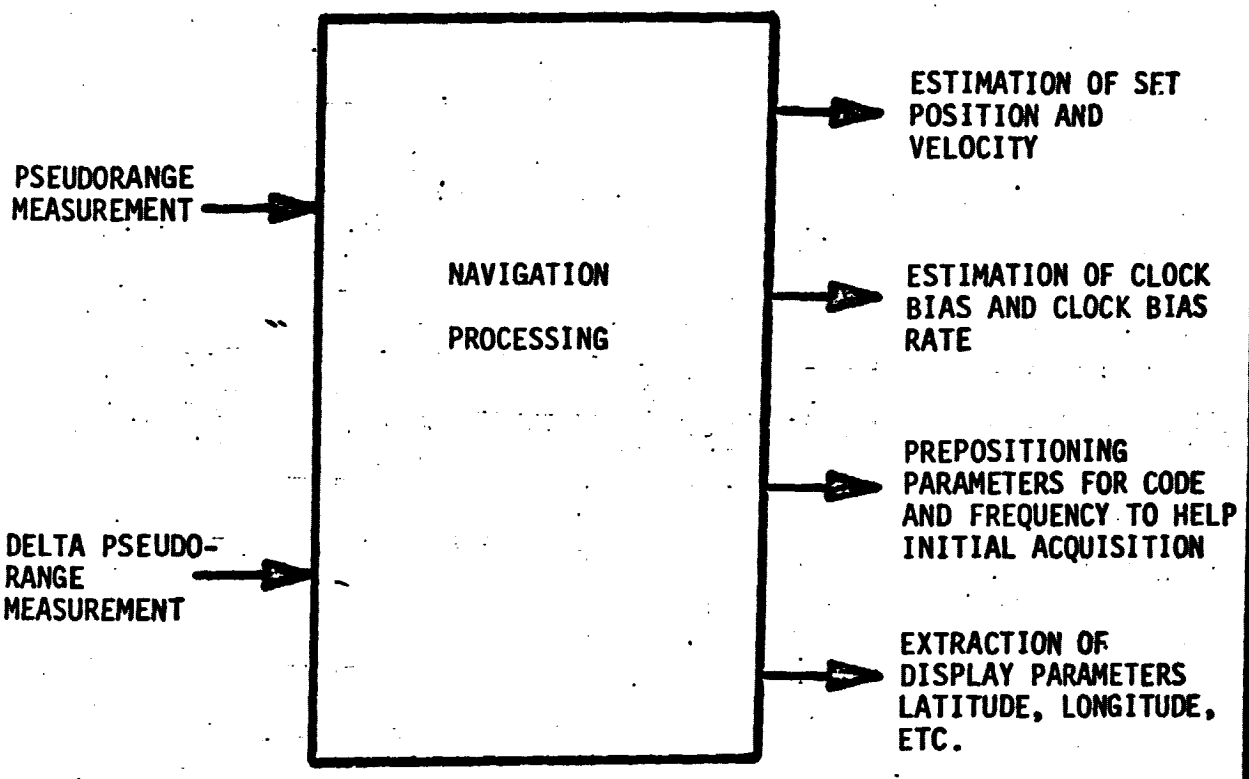

Figure 13b. Inputs/Outputs of Navigation Processing Software.

proper bit for current data word and space vehicle has arrived and accumulates 30 bit data word plus 2 parity bits from previous word. The outputs are the 32 bits of data word plus parity bits, word number and space vehicle number. The data processor is implemented in two levels which are: (1) bit accumulation into words and (2) word accumulation into coherent ephemeris or almanac page. Figure 14 shows the input and outputs of the data processor in a block diagram form.

4.3. Receiver Processor

The receiver processor (the software section of the receiver) has the following functions:

1. Receiver monitor and control.
2. Bit synchronization
3. Satellite data gathering.
4. Word/frame synchronization.
5. Parity checking.
6. Time and pseudorange management.

The receiver processor has several inputs and outputs which will be classified under three different interfaces listed below:

1. Receiver processor-receiver hardware interface.
2. Receiver processor-satellite sequence interface.
3. Receiver processor-navigation processor interface.

Each of these will be described in terms of the input/output (interface) block diagram. Fig. 15 depicts the interface between the receiver processor and receiver hardware.

1. Receiver Processor/Navigation Processor Interface

The outputs of navigation processor were described in general in the previous pages. Here we discuss those outputs of navigation

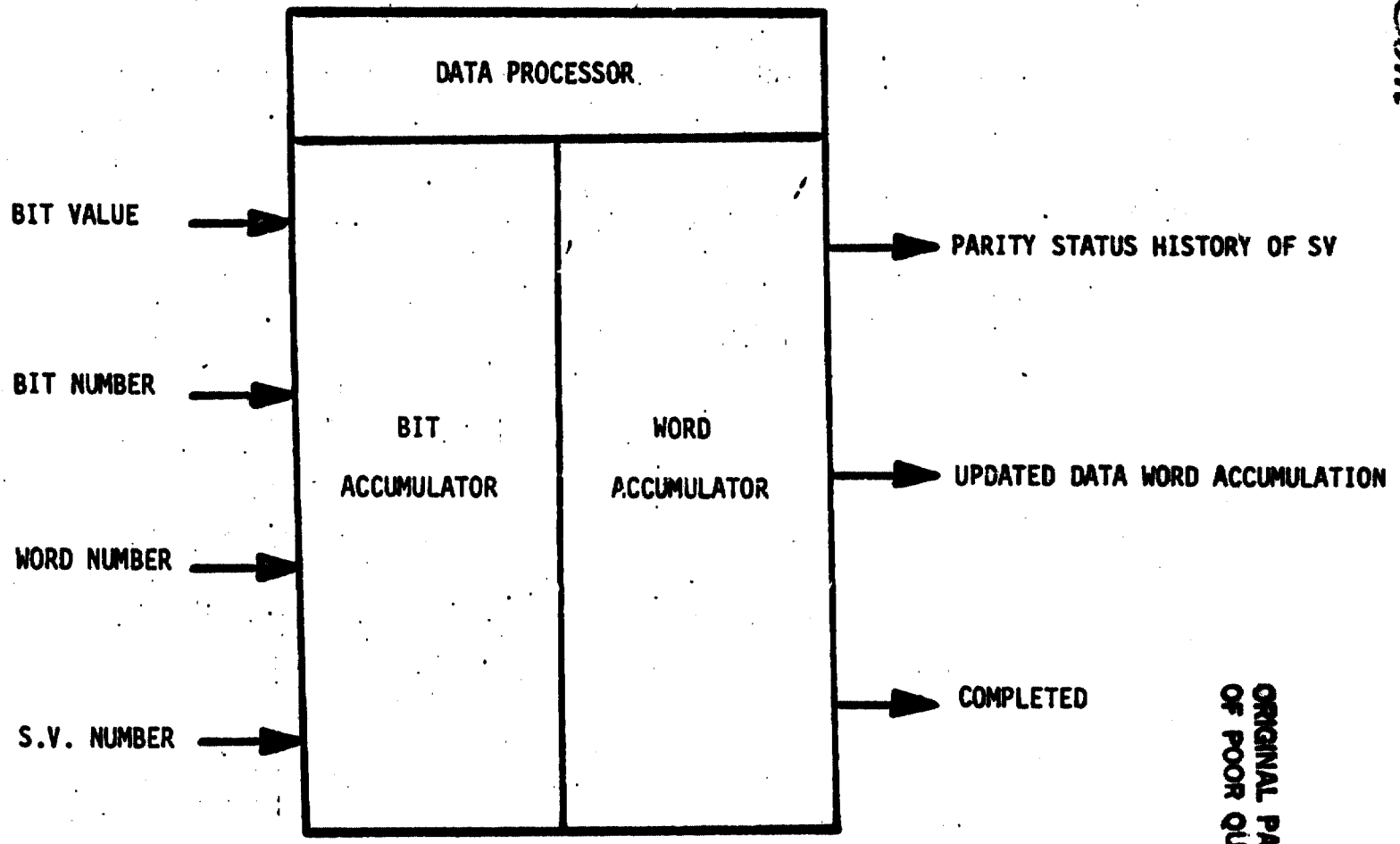

Figure 14. Inputs/Outputs of Receiver Set Data Processor Unit.

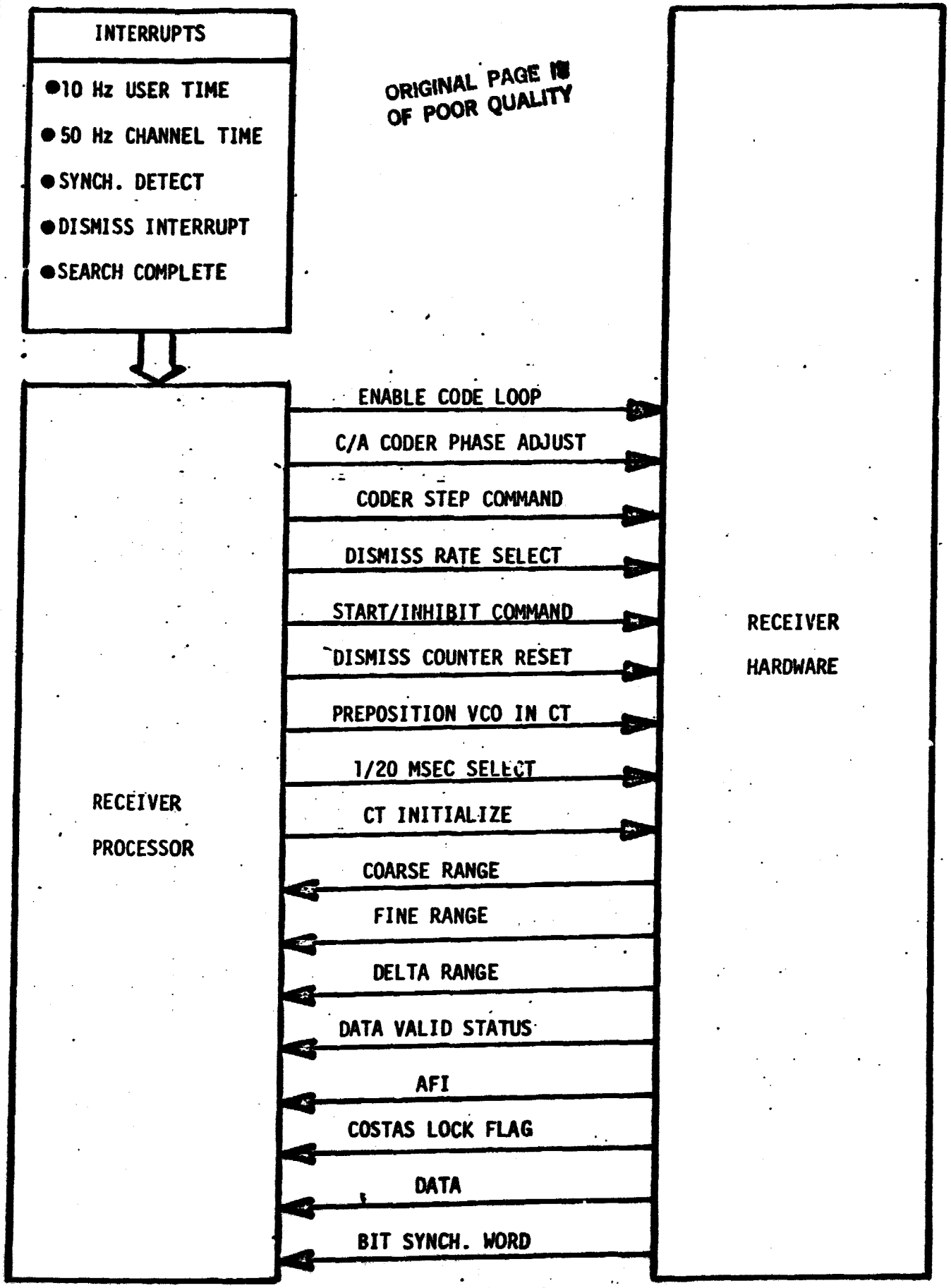

Figure 15. Receiver Processor/Receiver Hardware Interface.

processor which are necessary for the receiver processor to function. Figure 16 shows the interface between the receiver processor and navigation processor.

2. Receiver Processor/Satellite Sequencer Interface

The receiver processor needs several inputs from the satellite sequencer circuit to perform the following functions:

1. Space vehicle I.D. # for the next dwell.
2. Time duration necessary for the next dwell.
3. To enable next dwell mode such as initial acquisition, initial search, reacquisition, normal synch recovery, etc.

This interface is shown in Figure 17.

4.4 Control Display Unit Processor

This processor provides communications between GPS set user and navigation and receiver processing in the set. The display arrive funtions are:

1. Display navigation data.
2. Control operation of the set.
3. Indicate system status and health.
4. Insert waypoint coordinates.

Combined input/output for these form functions is shown in Figure 18.

Control Display Unit Inputs:

1. Latitude, longitude and altitude.
2. Distance to waypoint.
3. Bearing to waypoint.
4. Day and time.
5. Ground speed.
6. Time ground track.

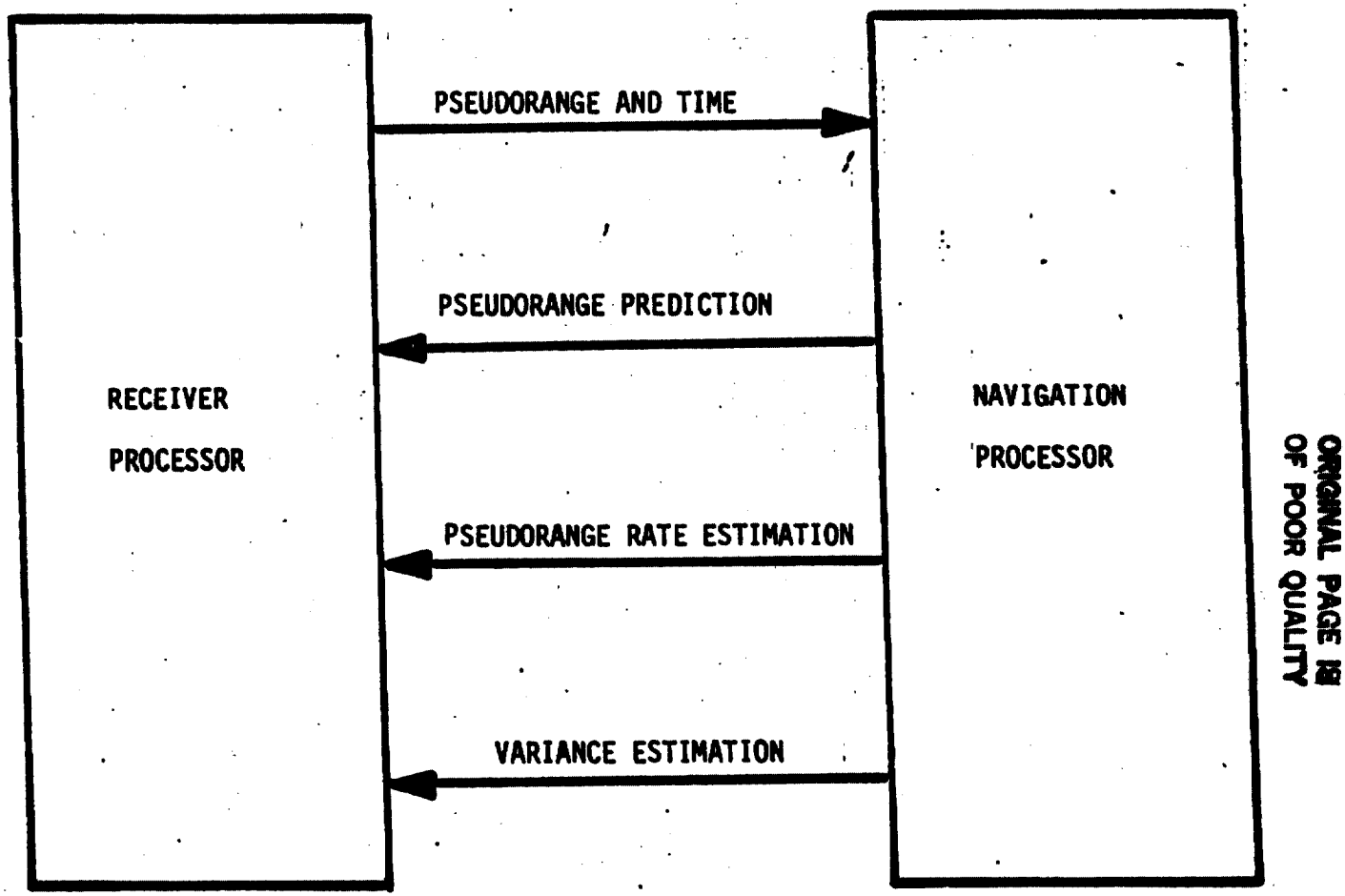

Figure 16. Receiver Processor/Navigation Processor Interface.

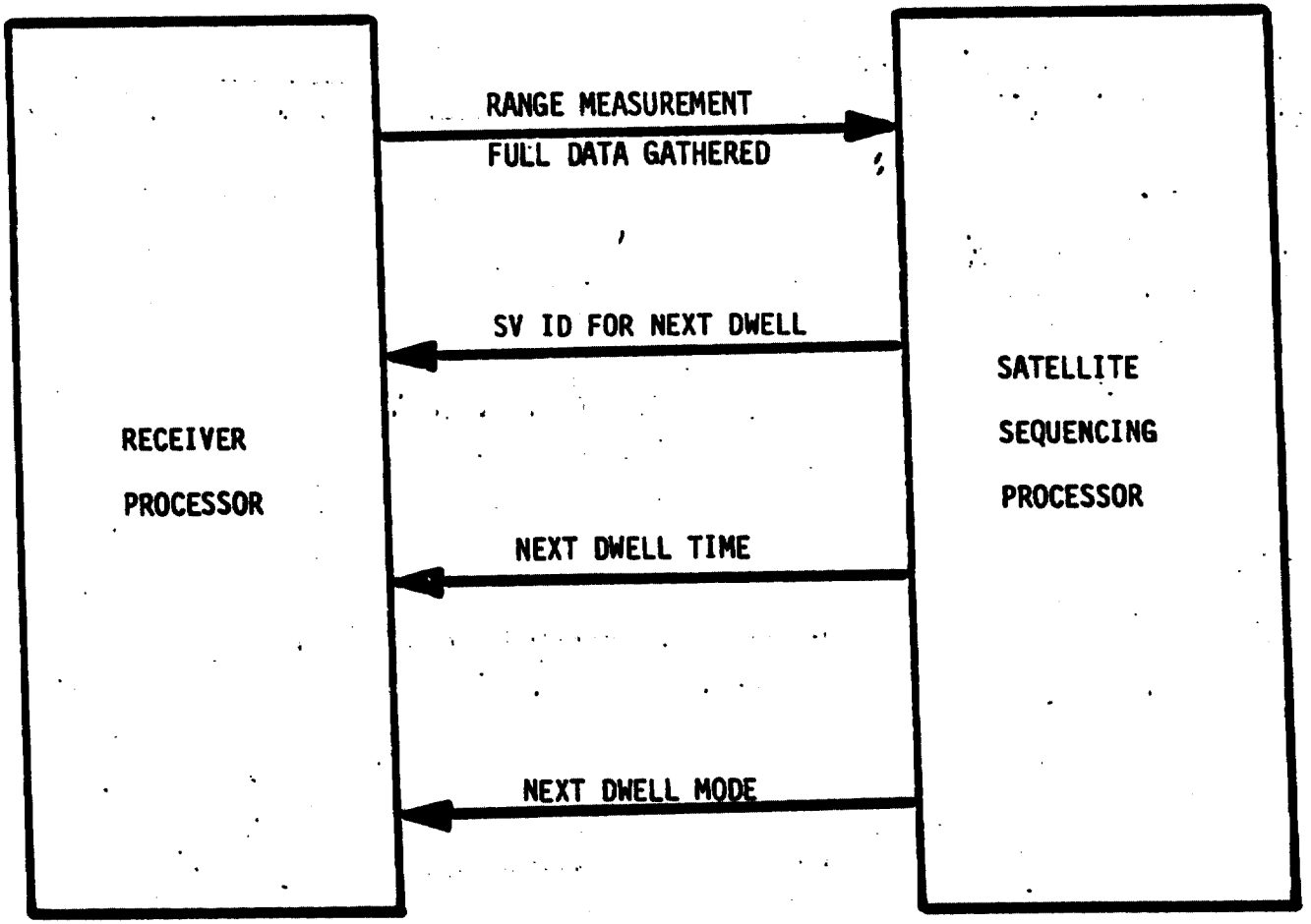

Figure 17. Receiver Processor/Satellite Sequencing Processor Interface.

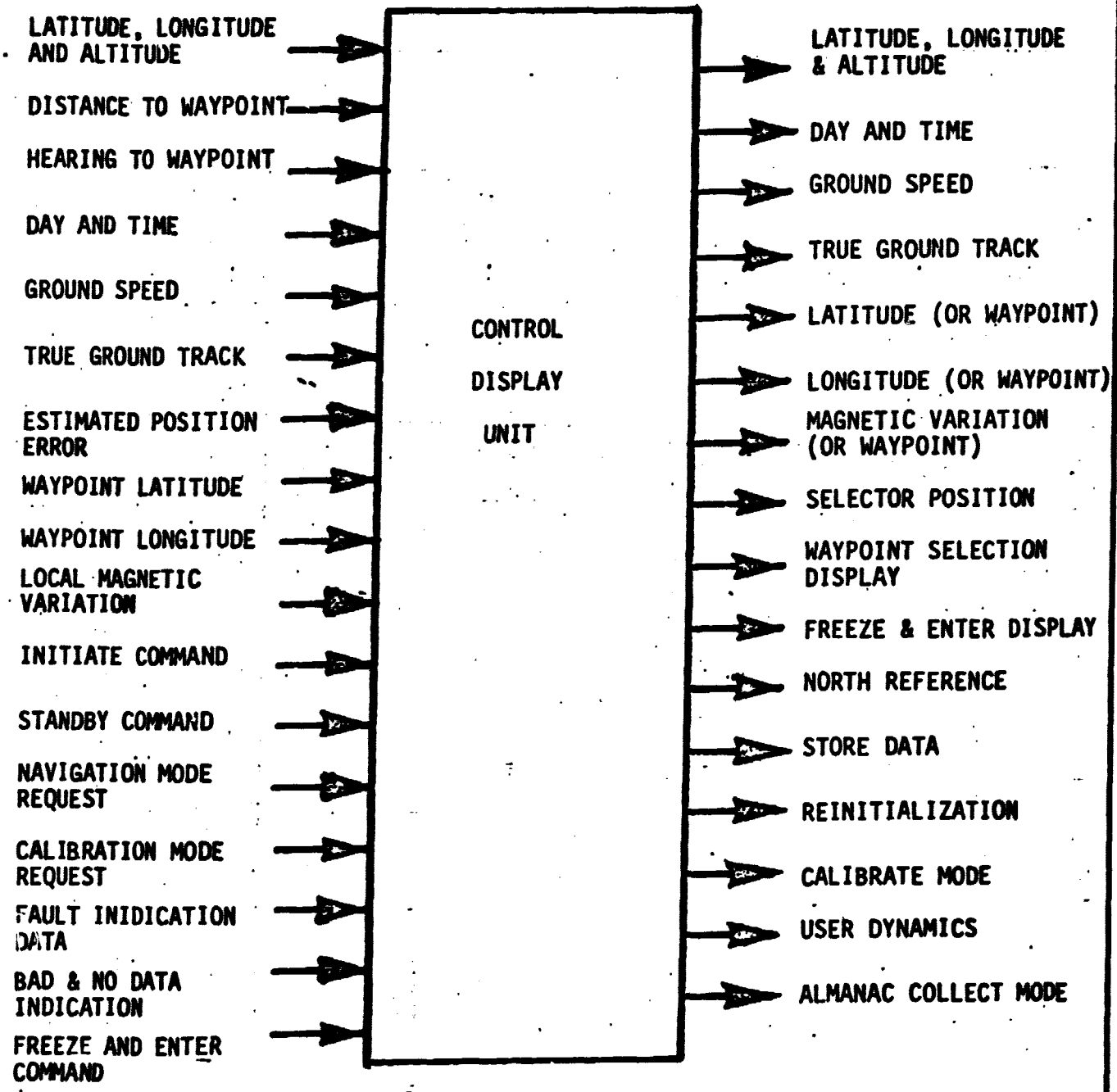

Figure 18. Input/Output of the Control Display Unit.

7. Estimated position error.
8. Waypoint latitude.
9. Waypoint longitude.
10. Local magnetic variation.
11. Initiate command.
12. Standby command.
13. Navigation mode request.
14. Calibration mode request.
15. Fault indication input from receiver.
16. Bad and no data indication command.
17. Frequency and enter command.

Control Display Unit Outputs:

1. Latitude, longitude and altitude.
2. Day and time.
3. Ground speed.
4. True ground track.
5. Latitude (of waypoint)
6. Longitude (of waypoint)
7. Magnetic variation (of waypoint).
8. Selector position.
9. Waypoint selection.
10. Freeze and enter.
11. North reference.
12. Store data.
13. Reinitialization.
14. Calibrate mode.
15. User dynamics.

16. Almanac collect mode.

5. Executive Processing

1. Provides time activates of user tasks.
2. Provides priority execution of tasks.
3. Enables the tasks that will be activated in the next scheduled loop.
4. Provides system time values.
5. Expands the minimum system throughput consistant with necessary functions and low memory requirements.
6. Nucleus of fundamental execution.
7. Provides for coherent transmission of data between tasks.

Figure 19 gives the information flow between the major function of the receiver set.

ZUSCP INFORMATION FLOW BETWEEN MAJOR FUNCTIONS

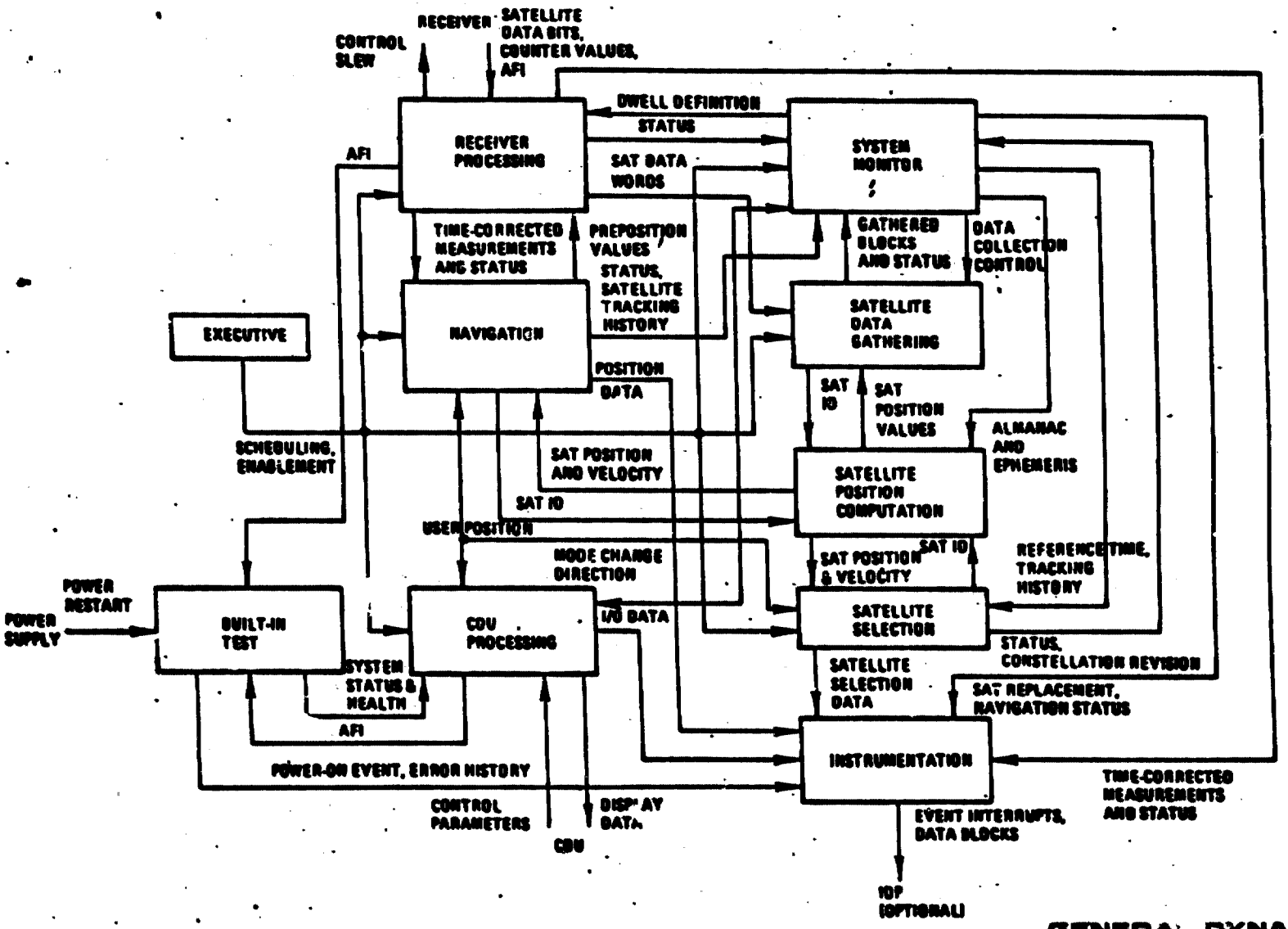

ORIGINAL PAGE IS OF POOR QUALITY

1177-7112

Figure 19.

GENERAL DYNAMICS
Electronics Division

REFERENCES

1. "Navstar Global Positioning System Z-set Design Review," prepared by General Dynamics Electronics Division, June 28,1976.

2. "Navstar Global Positioning System Set Z Preliminary Design Review," prepared by General Dynamics Electonics Division, July 26, 1976.

3. "Navstar Global Positioning Systems Phase I User Equipment Set Z Critical Design Review," prepared by General Dynamics Electronics Division, December 13, 1977.

4. GPS User Equipment Orientation Course Student Handbook, prepared by Magnavox.

ATTACHMENT II

ANTI-JAMMING PERFORMANCE OF SOC/EVA AND FREE-FLYER FORWARD AND RETURN LINKS

PREPARED FOR

NATIONAL AERONAUTICS AND SPACE ADMINISTRATION
LYNDON B. JOHNSON SPACE CENTER
HOUSTON, TX 77058

TECHNICAL OFFICER: WILLIAM TEASDALE

CONTRACT NO. NAS 9-16097

PREPARED BY

MICHAEL A. WHITE

LINCOM CORPORATION
P.O. BOX 2793D
PASADENA, CA 91105

MAY, 1982

TR-0582-1080

TABLE OF CONTENTS

LIST OF FIGURES

LIST OF FIGURES (continued)

LIST OF TABLES

LIST OF ACRONYMS

EVA: extravehicular activity

FH: frequency-hopped

FSK: frequency-shift keyed

MA: multiple-access

MFSK: M-ary frequency-shift keyed

NCL: noncoherent combining loss

RFI: radio frequency interference

SOC: Space Operations Center

FOREWORD

This technical report recommends a channel code and frequency hop rate for the proposed Space Operations Center (SOC) multiple-access communication links with extravehicular activities (EVAs) and free-flyers. The results are derived by analyzing the performance of the links in worst-case jamming.

This preliminary study of the SOC has been performed by LinCom Corporation for the National Aeronautics and Space Administration, Johnson Space Center. LinCom's activity was under the direction of Dr. William C. Lindsey.

1.0 INTRODUCTION

The susceptibility of the Space Operations Center (SOC)/ extravehicular activity (EVA) and free-flyer multiple-access (MA) links to jamming is very sensitive to the communication waveform design. Random hopping of the center frequency is one effective strategy for overcoming jamming. In this report, we analyze fast frequency hopping (FH) in both noise and tone jamming environments for the purpose of optimizing the design of the SOC/EVA and free-flyer forward and return waveforms. For each link, the maximum allowable jammer-to-signal power ratio is presented in Section 2 as a function of the jammer's frequency distribution, the required bit error probability (performance), and the characteristics of the waveform. The waveform characteristics and those of the SOC/EVA and free-flyer forward and return links are described in this section. The complete waveform for each of the links is recommended in Section 3.

1.1 Link Considerations

The SOC is the center of all communication between separate free-flyers and EVAs, in addition to its function as a relay for all signaling into and out of the SOC/EVA, free-flyer configuration. Free-flyers and EVAs use identical waveforms for communication with the SOC, in order to prevent an impractical hardware buildup in the SOC. We therefore have only two distinct systems; one for SOC transmission to the EVAs and free-flyers, and the other for the SOC/EVA, free-flyer return link.

A combination of EVAs and free-flyers may communicate simultaneously with the SOC. All of these users are required to be within 2000 kilometers (km) of the SOC, so any fading on either the

forward or return link is assumed to be slow, relative to the time required to transmit one symbol. The link users can be distributed anywhere within a 2000 km radius of the SOC, so the SOC must be capable of orienting its antenna beams in any direction.

Radio frequency interference (RFI), rather than thermal noise, is presumed to be the dominant cause of signal degradation on the forward and return links. In this report, we analyze the RFI effects on performance when the receiver is intentionally jammed. The jamming may cover a band of frequencies (partial band, or noise, jamming) in the signal spectrum, or it may be confined to a number of tones, as in multitone jamming. In both types of jamming, we assume that the jammer chooses the frequency distribution that will have the worst possible effect on link performance for a given received jammer power J. This worst-case jamming assumption implies that the free-flyers and EVAs may be jammed differently than the SOC.

1.2 Waveform Characteristics

LinCom was given several characteristics of the anti-jamming waveforms to be used on the MA forward and return links. The frequency of both the forward and return link communication waveforms will be randomly hopped to prevent any repeat back jammer from detecting the signaling pattern. Hopping forces any jammer to spread power over a number of possible signaling frequencies, instead of allowing him to concentrate his power on the center frequency. Fast frequency hopping has been proposed [1] for the SOC/EVA, free-flyer links, because the hops provide the most protection against worst-case jamming when they occur more than once during a symbol transmission. Due to the difficulty of maintaining the phase continuity of a symbol transmission

during a frequency hop, the receivers in the EVAs, free-flyers, and the SOC are to detect incoming signals noncoherently. All communication on both links will be synchronous, and users are to be frequency-division multiplexed onto the return link.

All of the baseband signals to be transmitted through the forward and return channels are digital. Although the expressions in Section 2 are derived without any numerical evaluation, we now quantify the data rate of the baseband signals. Video data and audio/command data are frequency multiplexed onto the forward link at 400 kilobits per second (Kb/s); the return link also consists of 400 Kb/s-video data, in addition to 50 Kb/s audio/telemetry data [1]. The best way of modulating these signals, for noncoherent communication over a large bandwidth is acknowledged to be frequency shift keying (FSK). For the SOC/EVA, free-flyer links, a 2 Gigahertz (GHz) bandwidth has been proposed [1] at the center frequency of 30 GHz. The carrier modulation was therefore chosen to be M-ary FSK (MFSK), where M is the number of baseband frequencies.

In this report, we complete the definition of the waveform by specifying the frequency hop rate, equal to the chip rate, on the forward and return links, and any channel coding to be performed. In Section 3, we present these characteristics for the forward and return links, based on analyses of worst-case jamming in Section 2.

1.3 Receiver Model

Before analyzing the anti-jam performance of the fast frequency-hopped, M-ary FSK waveform, we present a model of the forward and return link communication systems. The model includes only those operational characteristics which have an impact on the performance analysis of

Section 2.

On both the forward and return links, the M-ary FSK demodulator is a critical component of reliable communication. The M-ary FSK demodulator in each free-flyer and EVA, and in the SOC, is a noncoherent square-law detector in which the dehopped, squared envelopes e_{ij}^2 ($i=1,2,\ldots,m; j=1,2,\ldots,M$) of all m chips of each M-ary symbol are optimally combined in each of the M channels (Figure 1). In the jamming environment of the FH multiple-access (MA) channels, the optimal combination is simply a sum of all the squared envelopes, after all noise-free chips (only one of the M squared envelopes exceeds a small threshold) are amplified through automatic gain control [2]. The M-ary symbol that corresponds to the channel with the largest of the M sums is then chosen as the transmitted symbol.

Before the squared chip envelopes are added, they are clipped at the average received signal power S. This prevents the jammer from degrading performance by transmitting more power into one of the M filters than this clipped value. Although the clipping reduces the expected difference between the output of the correct filter and those of the (M-1) incorrect filters in partial band jamming, decision errors are not likely to occur more frequently than they do without clipping.

Given the total received jamming power J in either partial band or multitone jamming, link performance is best when the center frequency for a chip is randomly chosen from all the available frequency cells in the hopping bandwidth. If the center frequency is confined to tones which are separated by the baseband bandwidth and no baseband mixing is used, the multitone jammer can constantly jam one of the (M-1) incorrect baseband frequencies by separating his tones by the baseband

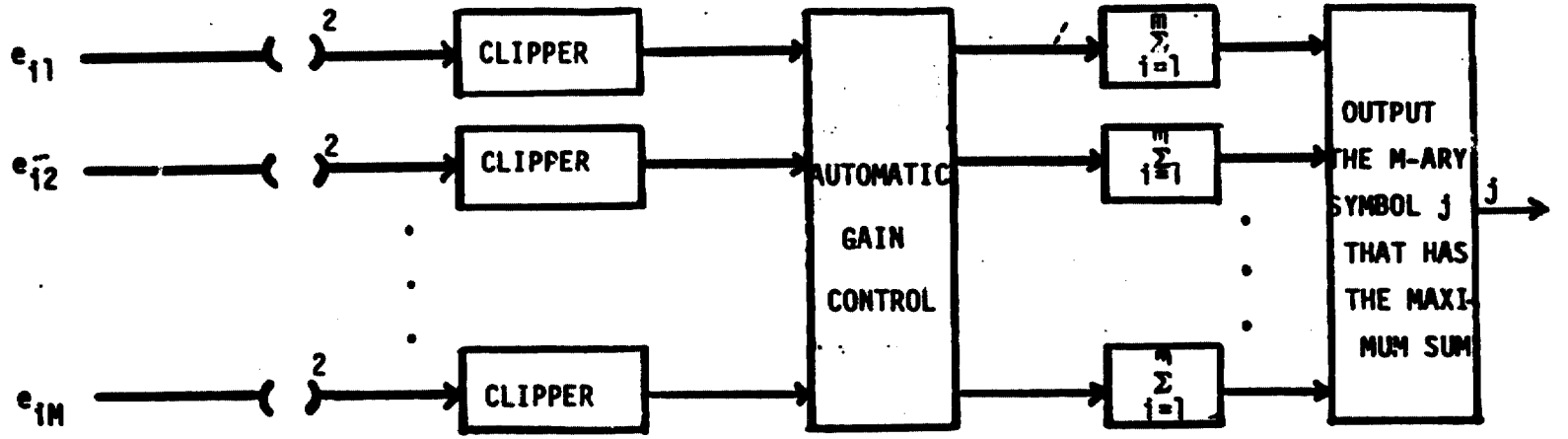

Figure 1. M-ary FSK Demodulator in Forward and Return Links.

bandwidth. We therefore assume that random hopping to any frequency cell is implemented in the hoppers and dehoppers of the FH MA forward and return links. The hop rate, or chip rate, of these units is the same on both links, because no more than one frequency synthesizer is permitted in each EVA and free-flyer.

2.0 PERFORMANCE AGAINST WORST-CASE JAMMING

A study of performance of the SOC/EVA, free-flyer MA links against worst-case jamming leads to the choice of channel code and chip rate for the forward and return link waveforms (Section 3). For a maximum bit error probability at a given data rate, the maximum jammer-to-signal power ratio (J/S) at the receiver, is very sensitive to the chip rate and, to a lesser extent, the code. In this section, we present expressions and graphs for J/S to measure anti-jam performance for various channel codes and chip rates.

We consider two different types of channel coding: block orthogonal and rate 1/2, dual-k convolutional. The 2^k-dimensional block orthogonal encoders map every distinct sequence of k data bits into a different M-ary (2^k-ary) symbol to be input to an M-ary FSK modulator. Dual-k encoders and decoders are slightly more complex. They require twice as much memory as 2^k-dimensional block orthogonal encoders and decoders, for the purpose of storing the previous k-bit input (Figure 2). Encoding each k-bit input by combining it with the previous one, gives rate 1/2, dual-k convolutional codes a coding gain over block orthogonal codes.

The coding gain in allowable J/S of the dual-k codes can be observed in the graphs of J/S_t that are derived in this section. Beside the type of coding, J/S is a function of the chip rate R_h, the number k

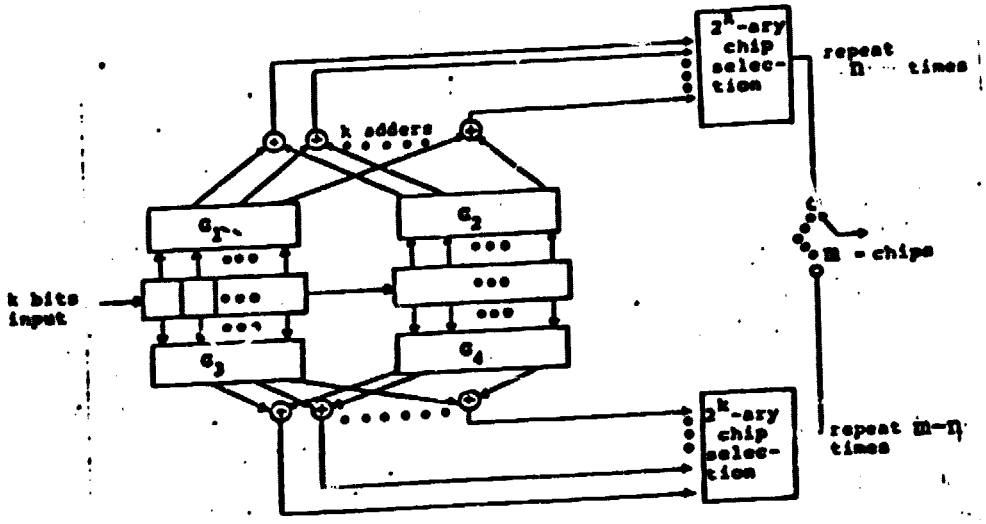

Figure 2. Rate 1/2, Dual-k Encoder.

of data bits per coded symbol, the data rate R_b, the maximum bit error probability P_b, the frequency-hopping bandwidth W, and the type of worst-case jamming, either partial band (noise) or multitone. Since R_b = 400 Kb/s for all data on the forward link, this link will be analyzed first. Most of the results of this analysis can be directly transferred to the return link, where data rates of 50 and 400 Kb/s are studied. On both links, bit error probability performance is either 10^{-3} or 10^{-5} and $2 \leq k \leq 5$.

2.1 Forward Link

As described in 1.2, the SOC-to-EVA (and free-flyer) link is a fast frequency-hopped, 2 GHz channel used for digital video and audio/command data, both of which are frequency multiplexed at 400 Kb/s. In focusing on the jamming susceptibility of the link, we neglect any performance degradation due to other sources, e.g., synchronization loss, equipment noise, and thermal noise. Because the chips of each symbol are optimally combined by the MFSK demodulators in the EVAs and free-flyers, an M-ary symbol is detected erroneously only when the worst-case jammer succeeds in jamming every chip.

The worst-case partial band jammer jams a chip by reducing the output chip envelope of the signaled filter in the demodulator, through phase cancellation, below the output of at least one other filter. Symbol errors due to phase cancellation can occur even when the jammer gets less total power through all filters than the signal power S. Viterbi and Jacobs [2] have shown that partial band jamming is most likely to cause such a detection error when its frequency distribution is two-level, i.e., the jammer spreads his total power J evenly over a fraction ρ of the 2 GHz hopping bandwidth, leaving the remainder of the

band free of any jamming. The worst-case fraction ρ increases as the chip rate R_h increases because this means the signal energy per chip S/R_h is decreasing, while the probability of hopping to a particular frequency during a symbol transmission is rising. Eventually, ρ reaches 1 and the jamming is broadband, covering the entire hopping band.

For block orthogonal M-ary FSK, Trumpis [3] has given an exact characterization of the bit error probability P_b when $\rho < 1$, and we can apply Lindsey's result [4] to the broadband jamming case. From [5], the maximum allowable jammer-to-signal power ratio $(J/S)_{block}$ for block-orthogonally coded M-ary FSK is

$$\left(\frac{J}{S}\right)_{block} = \frac{W}{10^{A(M)}R_h}\left[\frac{P_b}{K''(M)}\right]^{\frac{1}{m}}, \quad \rho < 1 \qquad (1a)$$

$$\left(\frac{J}{S}\right)_{block} = \frac{Wk}{2R_b z}, \quad \rho = 1 \qquad (1b)$$

W: frequency hopping, or spread, bandwidth

m: number of chips/M-ary symbol (or diversity)

$K''(M)$ and $A(M)$: unitless constants, dependent only on M

z is half the M-ary symbol energy-to-noise density ratio $\left(\frac{SWk}{2JR_b}\right)$ that satisfies

$$P_b = 2^{k-1-m}e^{-z}\sum_{i=0}^{m-1}\left(\frac{1}{2}\right)^i L_i^{(m-1)}(-z) \qquad (2)$$

where m, the diversity, must be a positive integer. $L_i^{(m-1)}(\cdot)$, $i = 0,1,2,\ldots,m-1$, is the i-th generalized Laguerre polynomial of order (m-1) [6], defined recursively by

$$L_0^{(m-1)}(-x) = 1$$

$$L_1^{(m-1)}(-x) = x+m \qquad (3)$$

$$L_i^{(m-1)}(-x) = \frac{1}{i}(x+m+2i-2)L_{(i-1)}^{(m-1)}(-x) - \frac{2}{i}(m+i-2)L_{(i-2)}^{(m-1)}(-x),\ i=2,\ldots,m-1$$

The maximum allowable J/S given by (1) is plotted in Figs. 3 and 4 as a function of R_h for $P_b = 10^{-3}$ and 10^{-5}, respectively. Note that the diversity m is directly proportional to R_h:

$$m = \frac{kR_h}{R_b} \qquad (4)$$

Since $P_b/K''(M) \ll 1$, the exponent 1/m in (1a) accounts for the rapid increase in J/S with R_h, until the R_h factor in the denominator of (1a) begins to dominate and J/S steadily decreases.

The decrease is due to a progressively larger loss in the noncoherently combined signal chip envelopes, as the M-ary symbol is divided into shorter chips. Before this effect (called noncoherent combining loss [NCL]) dominates, diversity effectively alleviates even worst-case partial band jamming. The peaks of the curves (Figs. 3 and 4) always occur in the region where $\rho < 1$, hence (1a) is in effect.

Rate 1/2, dual-k convolutional coding of each k-bit input to the 2^k-ary FSK modulator in the SOC, provides more protection against worst-case partial band jamming than block orthongonal coding of the k-bit inputs. Again, we present two expressions for the maximum allowable J/S at the receiver, depending on whether the jamming is strictly partial band ($\rho<1$) or broadband ($\rho=1$). From [7], rate 1/2, dual-k coding yields a gain G(m) over 2^k-ary block orthogonal coding of

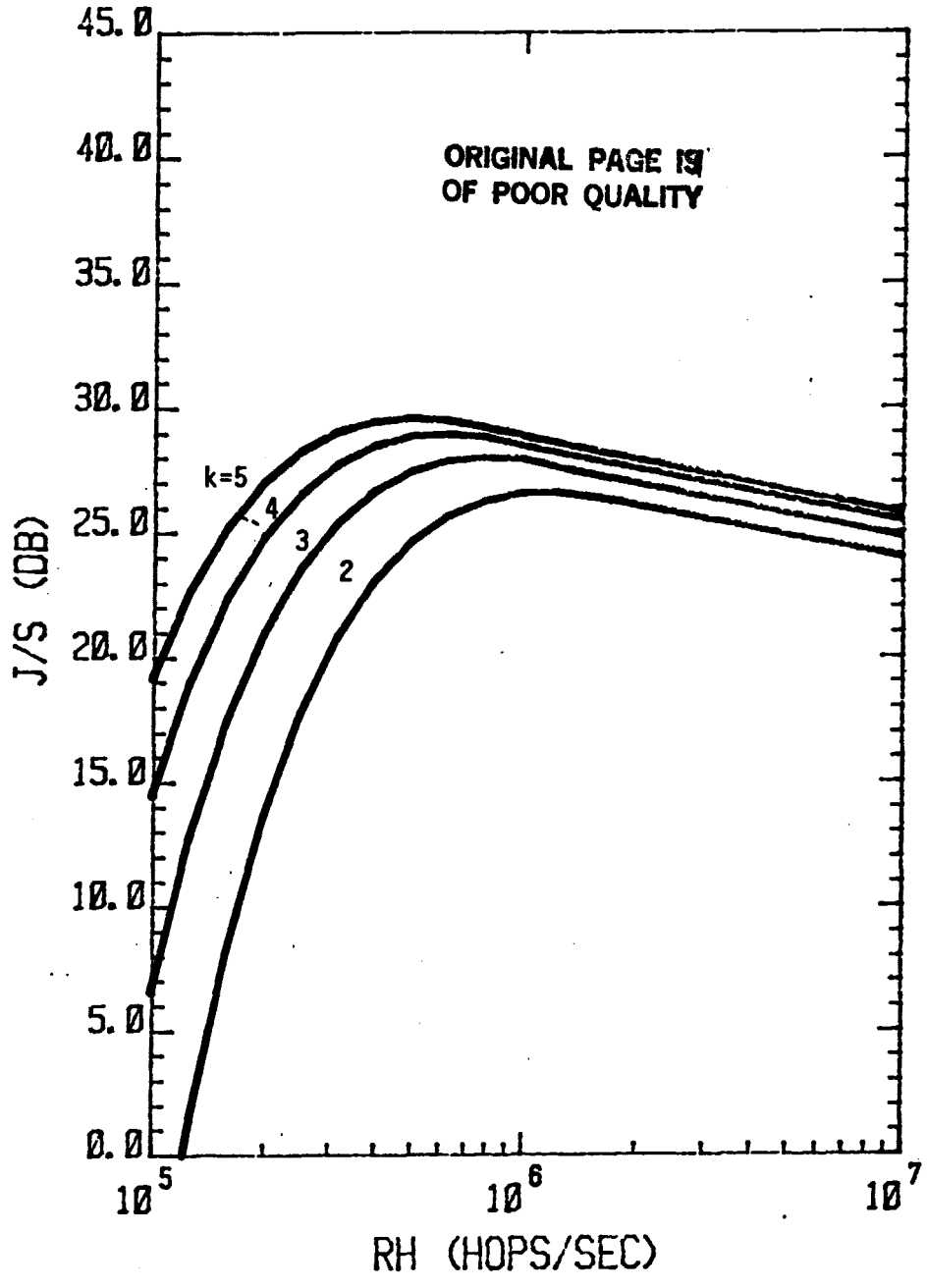

Figure 3. Maximum Allowable Jammer-to-Signal Power Ratio (J/S) in Worst-Case Partial Band Noise Jamming for Block-Orthogonally Coded 2^k-ary FSK, W = 2 GHz, R_b = 400 Kb/s, $P_b = 10^{-3}$.

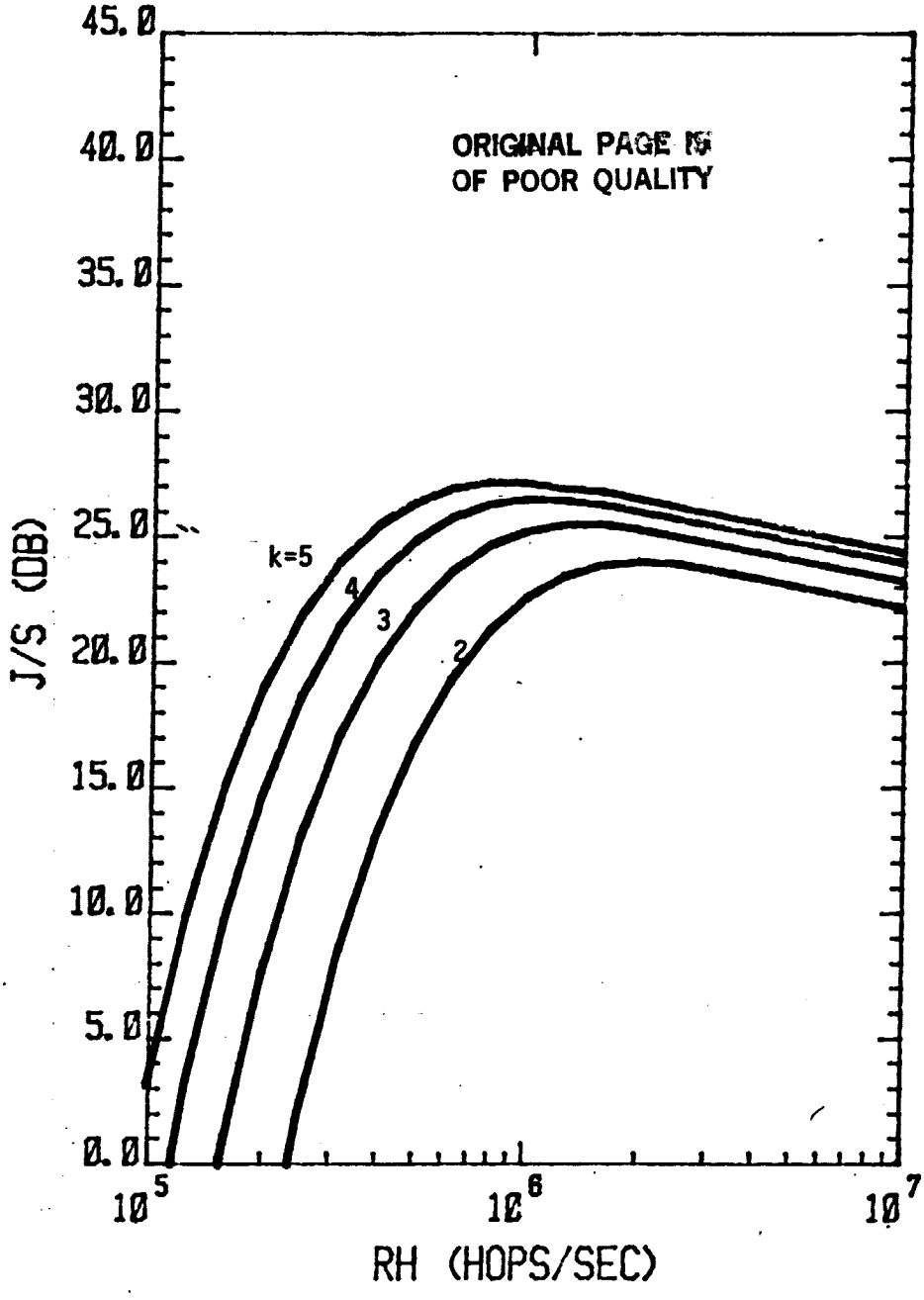

Figure 4. Maximum Allowable J/S in Worst-Case Partial Band Noise Jamming for Block-Orthogonally Coded 2^k-ary FSK, W = 2 GHz, R_b = 400 Kb/s, $P_b = 10^{-5}$.

$$G(m) \equiv \frac{(J/S)_{dual\text{-}k}}{(J/S)_{block}} \doteq \left(\frac{2^{k-1}\delta(P_b)}{P_b}\right)^{1/m} \qquad (5)$$

where $\delta(P_b)$ is given implicitly by [8]

$$P_b = \frac{2^{k-1}\delta^2(P_b)}{[1-2\delta^{1/2}(P_b)-(2^k-3)\delta(P_b)]^2} \qquad (6)$$

The maximum allowable J/S for dual-k coding $(J/S)^*_{dual\text{-}k}$ is derived by substituting (1) into (5) and solving for $(J/S)_{dual\text{-}k}$. This gives

$$(J/S)^*_{dual\text{-}k} \doteq \begin{cases} \dfrac{WG(m)}{10^{A(M)}R_h}\left(\dfrac{P_b}{K''(M)}\right)^{1/m}, & \rho < 1 \qquad (7a) \\ \dfrac{WkG(m)}{2R_b z}, & \rho = 1 \qquad (7b) \end{cases}$$

where ρ is the worst-case band fraction for block orthogonal coding.

Approximation (7) is plotted in Figures 5 and 6 for bit error probabilities of 10^{-5} and 10^{-3}, respectively. The coding improvement G(m) diminishes as m becomes large and the right hand side of (5) approaches 1. This effect coincides with the dominance of NCL and, equivalently, the R_h factor in the denominator of (7a). In the broadband (ρ=1) or linear region of the plots, z increases with R_h, and there is no gain from either diversity or dual-k coding. The peaks of the curves are again in the strictly partial band (ρ<1) region, where the coding gain G(m) of dual-k codes over 2^k-ary block orthogonal codes is large.

Unlike partial band or noise jamming, the worst distribution of a given total tone jamming power J at the EVA or free-flyer receiver is

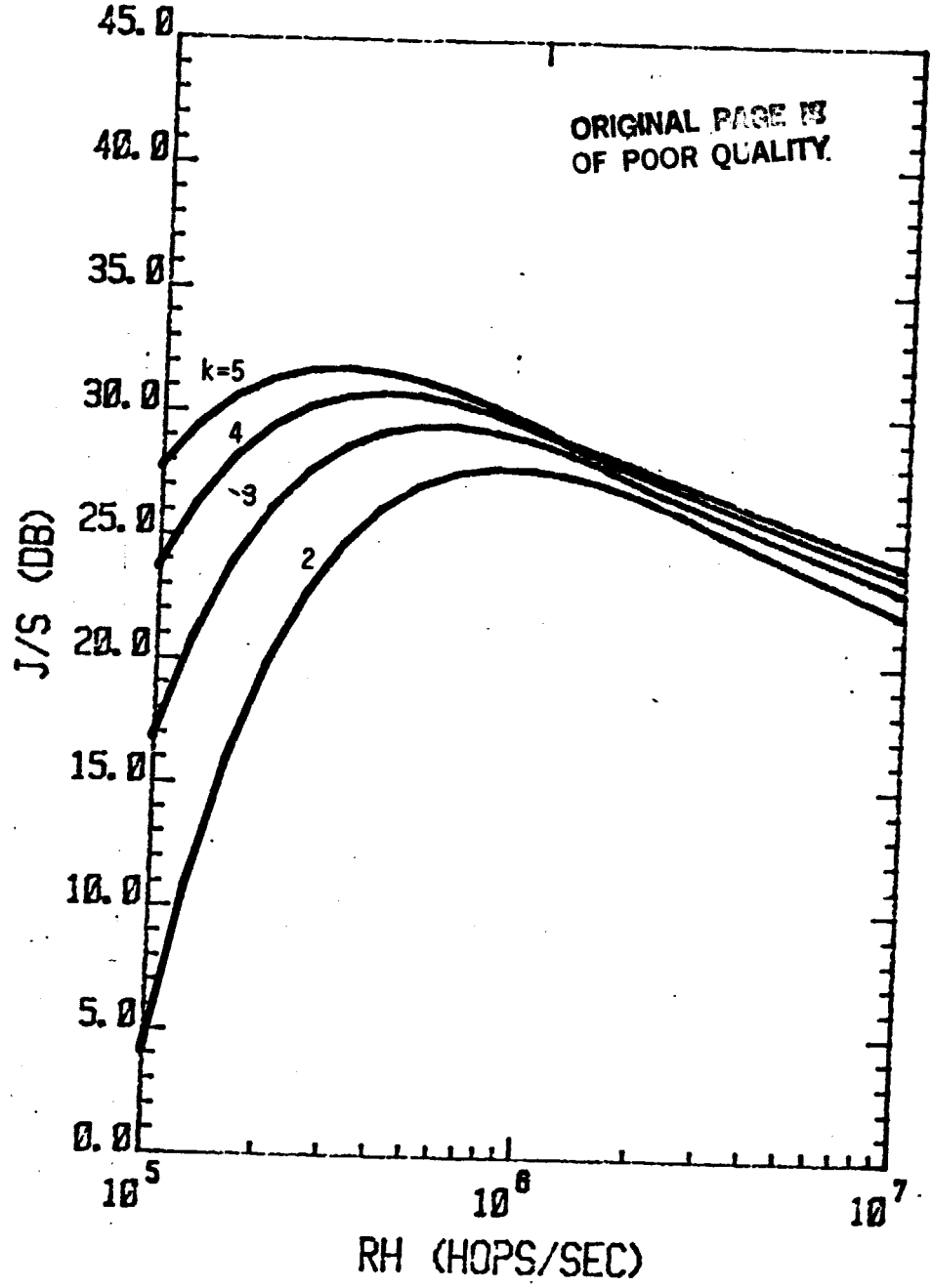

Figure 5. Maximum Allowable J/S in Worst-Case Partial Band Noise Jamming for Rate 1/2, Dual-k Coded 2^k-ary FSK, W = 2 GHz, R_b = 400 Kb/s, $P_b = 10^{-5}$.

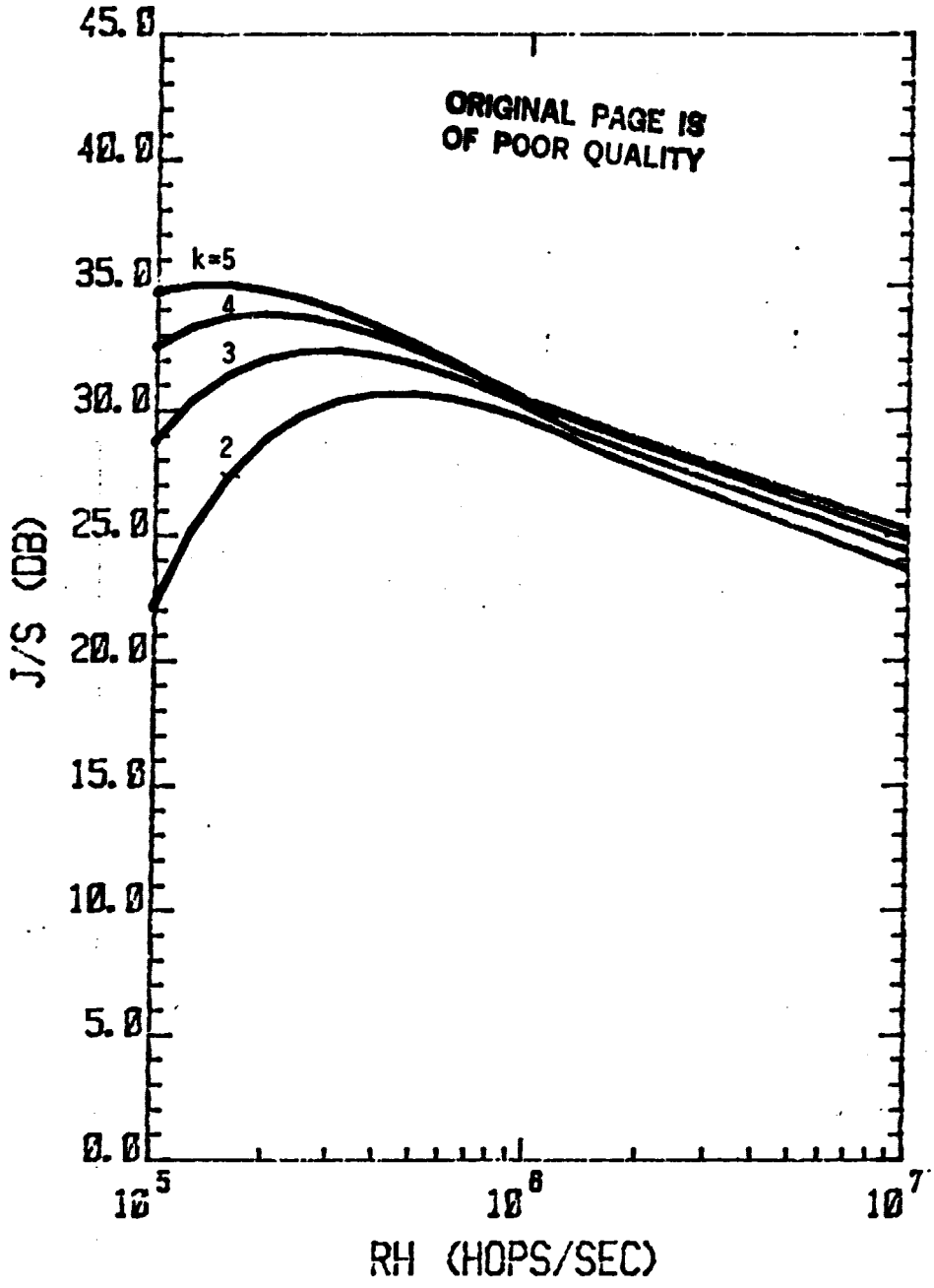

Figure 6. Maximum Allowable J/S in Worst-Case Partial Band Noise Jamming for Rate 1/2, Dual-k Coded 2^k-ary FSK, W = 2 GHz, R_b = 400 Kb/s, P_b = 10^{-3}.

tones of equal power j [2]. The jammer therefore has to choose between a few high-power tones or many tones of less individual power, distributed uniformly throughout the hopping bandwidth W. In the worst case, each of the jamming tones coincides with one of the available hopping tones which we assume to be separated by the chip rate R_h.

Optimal combining, at the MFSK demodulator of every EVA and free-flyer, requires any jammer to jam every chip of a transmitted M-ary symbol. Unlike the partial band jammer, the multitone jammer may jam chips in two different ways. In addition to creating symbol detection errors through signal phase cancellation, jamming tones may also overpower the signal without affecting its phase. The relative probabilities of these two types of errors determines the tradeoff between the number of jammer tones and their power J.

If a jamming tone is to overpower the signal tone without affecting its phase, the power j in each jamming tone at the receiver must be greater than or equal to the received signal power S. Without phase interference, the signaled filter of the M-ary FSK demodulators in the EVAs and free-flyers will have the largest output, unless another filter is jammed with power S. Since each squared chip envelope is clipped at S, the tone jammer sets j equal to S when his strategy is to overpower the signal. The tone power j does not necessarily equal S, however, when phase cancellation is part of the jamming strategy. Phase cancellation can cause detection errors when j is as small as S/4, but only if the signaled filter and at least one other filter of the MFSK demodulator are jammed. A jamming tone is k times more likely to strike any one of the filters in the demodulator than it is to enter the signaled filter, where phase interference occurs.

We therefore assume that the worst-case multitone jammer attempts to overpower the signal, rather than interfere with its phase. For $k \geq 2$, the tone-overpowering strategy is clearly superior for the jammer, unless the diversity (hops/k bits) is large. As the diversity increases the separation between jamming tones decreases and the distinction between the two strategies fades. Thus, for all diversities, the worst-case frequency distribution at the EVA and free-flyer receivers is assumed to be J/S jamming tones, of individual power S, uniformly separated in the hopping bandwidth W.

To plot the maximum allowable J/S as a function of the hop rate R_h, we begin with a union bound on link performance in the worst-case multitone jamming environment. The actual probability P_B that a block-orthogonally encoded bit will be decoded incorrectly is [8]

$$P_B < 2^{k-1}\left(\frac{JR_h}{SW}\right)^m \tag{8}$$

For the required maximum bit error probability P_b, we must have

$$P_B < P_b \tag{9}$$

(9) is always true if we substitute the maximum P_B, hence the maximum J/S, from (8).

$$2^{k-1}\left(\frac{JR_h}{SW}\right)^m < P_b \tag{10}$$

We now solve (10) for the maximum allowable J/S for block orthogonal coding

$$\left(\frac{J}{S}\right)_{block} > \frac{W}{R_h}\left(\frac{P_b}{2^{k-1}}\right)^{1/m} \qquad (11)$$

Equality in (11) is plotted in Figures 7 and 8 for required bit error probabilities of 10^{-3} and 10^{-5}, respectively. The shapes of the curves are similar to those for partial band jamming (Figs. 3 and 4), but NCL at high diversity degrades anti-jam performance faster than it does in the partial band case. In fact, increasing k, the number of bits per M-ary symbol or codeword, offers very little performance improvement in this region.

The maximum allowable J/S for rate 1/2, dual-k coding is derived by solving (5) for $(J/S)_{dual\text{-}k}$ and substituting the equality in (11).

$$(J/S)_{dual\text{-}k} \doteq \frac{W}{R_h}\left[\delta(P_b)\right]^{1/m} \qquad (12)$$

where $\delta(P_b)$ is again given by (6). (12) is plotted in Figs. 9 and 10 for $P_b = 10^{-5}$ and $P_b = 10^{-3}$, respectively. As in partial band jamming, the gain in J/S of dual-k coding over block orthogonal coding, is large for small diversity, but deteriorates as the hop rate R_h increases. Also, the value of k makes little difference when R_h is large. The peaks of all the curves for multitone jamming (Figs. 7-10) occur at a small R_h, where a fraction of the available hopping tones are jammed.

2.2 Return Link

The EVA (or free-flyer)-to-SOC link is very similar to the forward link. EVAs and free-flyers transmit frequency-multiplexed, fast frequency-hopped, MFSK video and audio/telemetry data in a 2 GHz hopping bandwidth. As on the forward link, the video data rate is 400 Kb/s; the

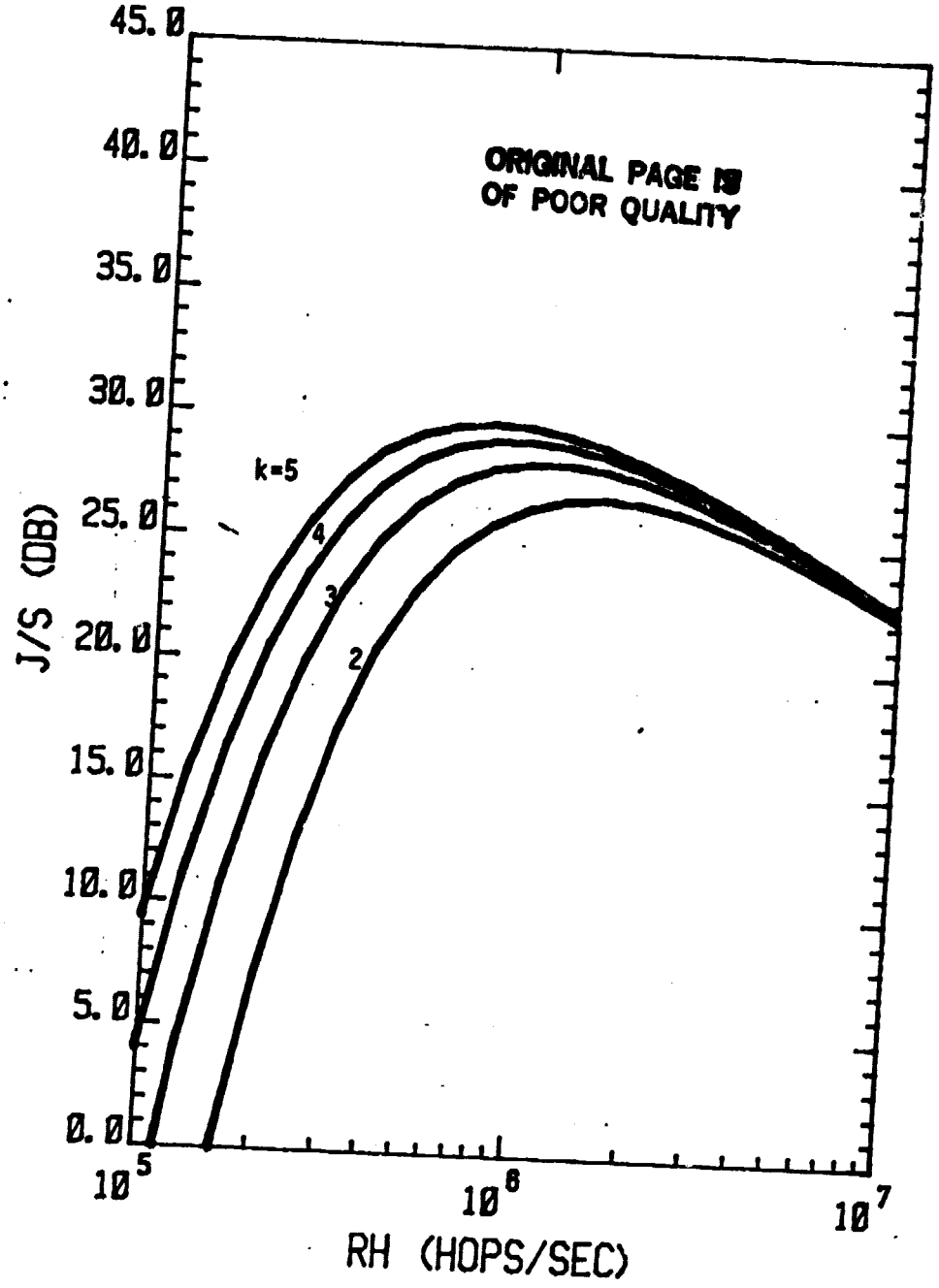

Figure 7. Maximum Allowable Jammer-to-Signal Power Ratio (J/S) in Worst-Case Multitone Jamming for Block-Orthogonally Coded 2^k-ary FSK, W = 2 GHz, R_b = 400 Kb/s, P_b = 10-3.

ORIGINAL PAGE IS
OF POOR QUALITY

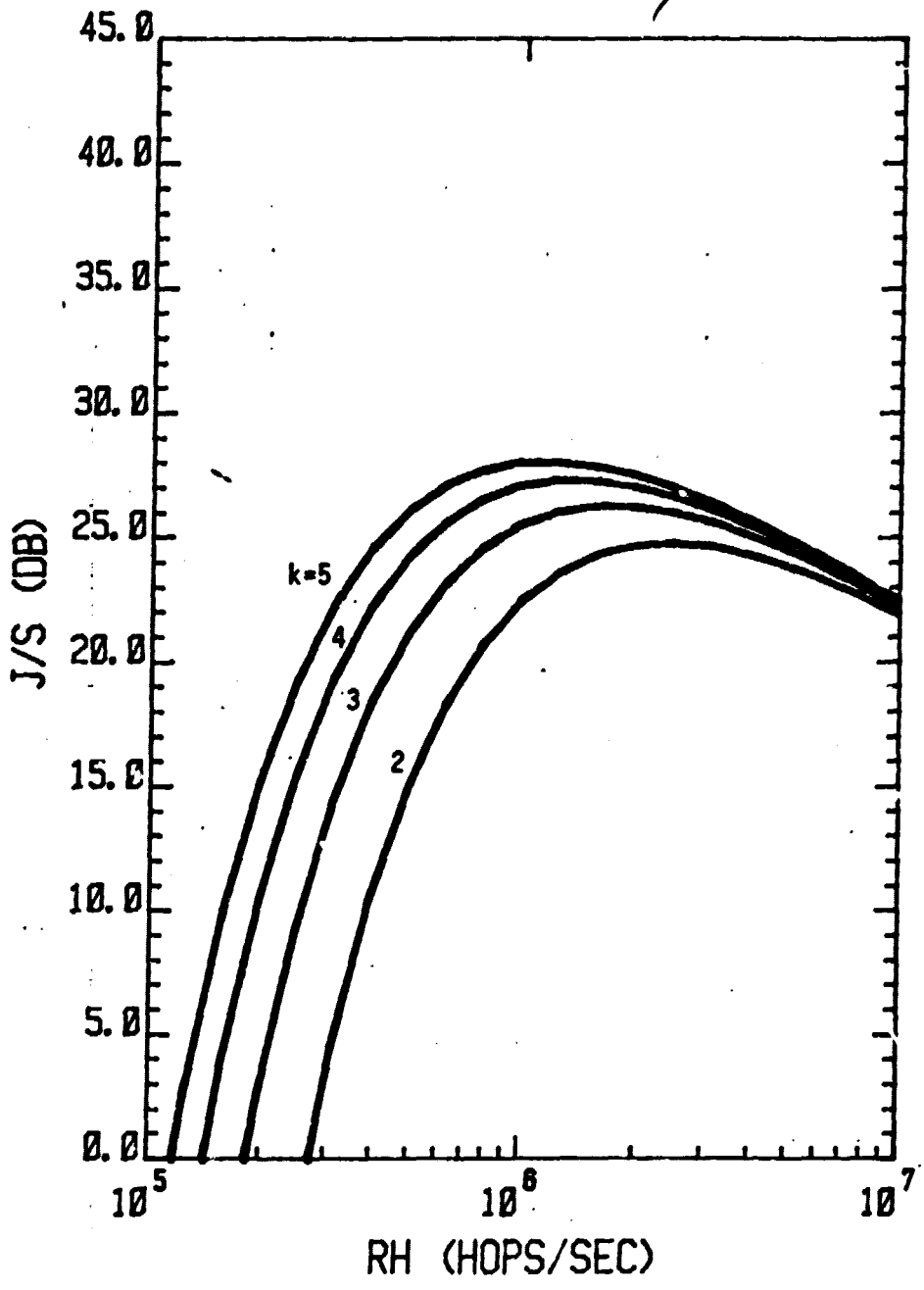

Figure 8. Maximum Allowable J/S in Worst-Case Multitone Jamming for Block-Orthogonally Coded 2^k-ary FSK $W = 2$ GHz, $R_b = 400$ Kb/s, $P_b = 10^{-5}$.

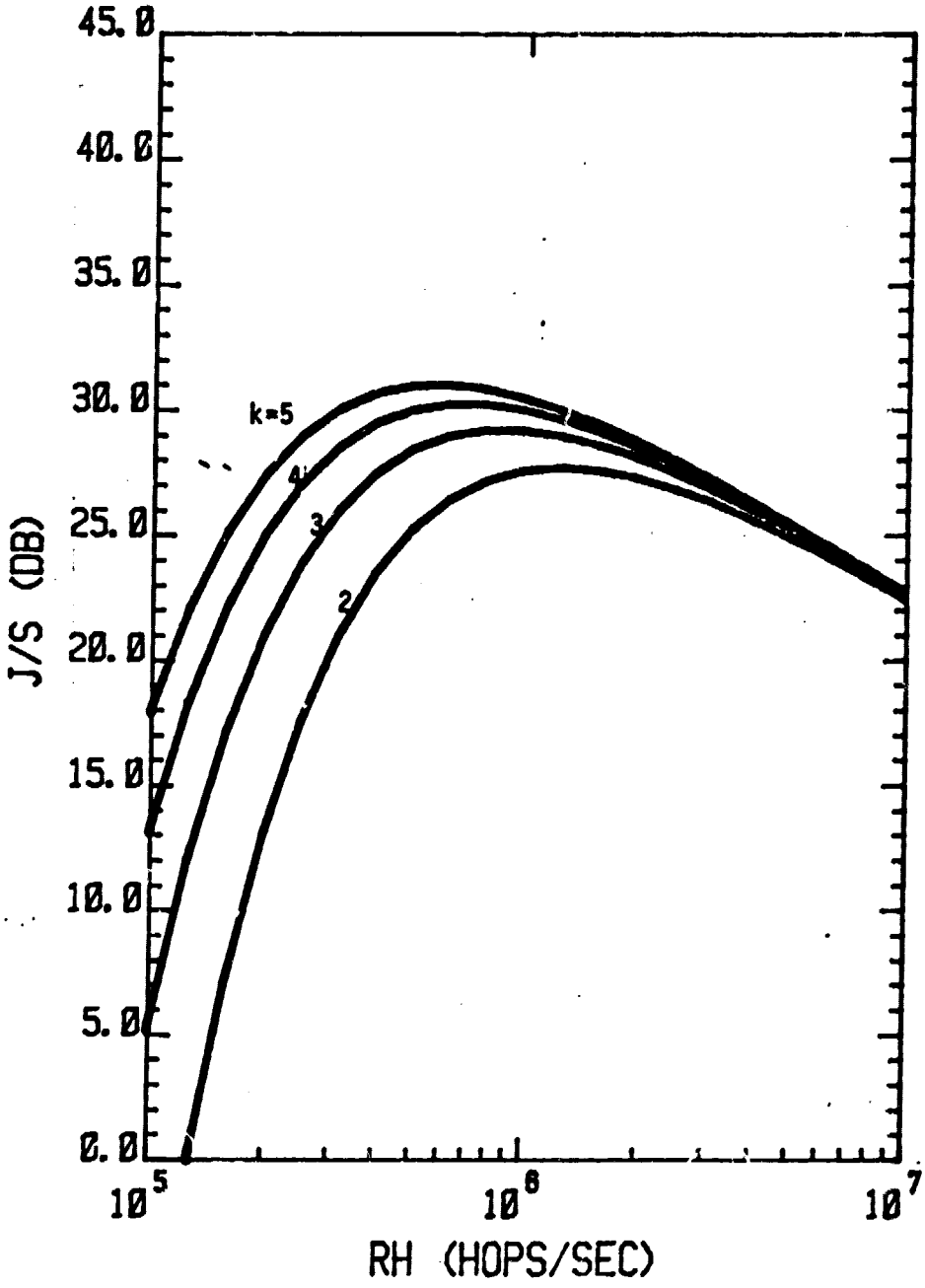

Figure 9. Maximum Allowable J/S in Worst-Case Multitone Jamming for Rate 1/2, Dual-k Coded 2^k-ary FSK, W = 2 GHz, R_b = 400 Kb/s, P_b = 10^{-5}.

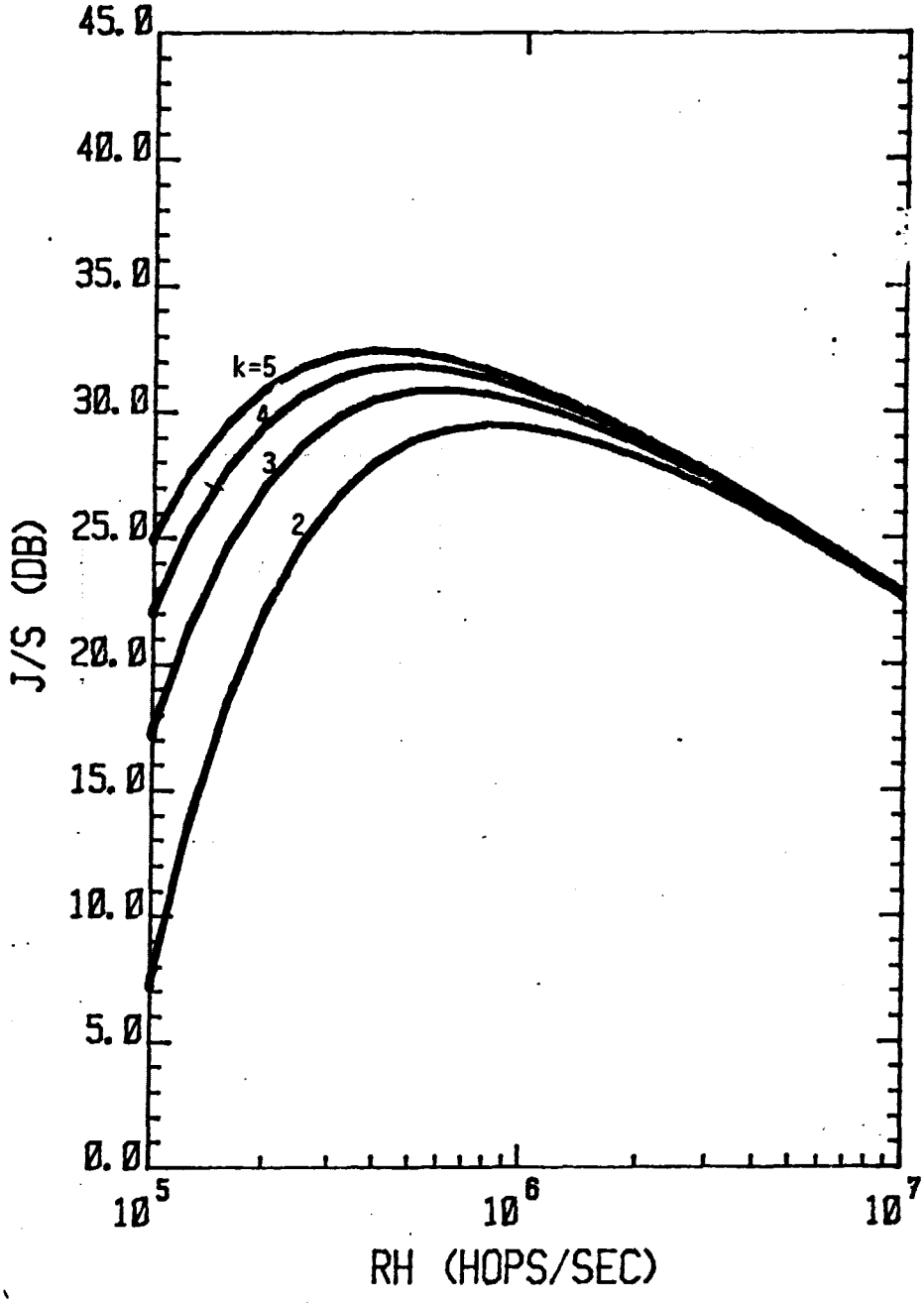

Figure 10. Maximum Allowable J/S in Worst-Case Multitone Jamming for Rate 1/2, Dual-k Coded 2^k-ary FSK, W = 2 GHz, R_b = 400 Kb/s, P_b = 10^{-3}.

audio/telemetry data rate, however, is only 50 Kb/s. Aside from this data rate variation, the characteristics and analysis of the return link are identical to those of the forward link. Hence the anti-jamming performance results of 2.1 (Figs. 3-10) apply directly to the video return channel.

In addition to these results, the anti-jam performance in allowable J/S can be presented as a function of the data rate R_b at a given frequency hop, or chip, rate R_h. As expressions (1), (7), (11) and (12) indicate, J/S is a decreasing function of R_b (Fig. 11) for fast frequency hopping. Therefore the allowable J/S on the 50 Kb/s audio/telemetry return channels is greater than that on the 400 Kb/s channels. J/S begins to level off, however, as R_b drops more than an order of magnitude below R_h and noncoherent combining loss (NCL) offsets the diversity gain.

3.0 RECOMMENDATIONS

Channel codes and a common frequency hop rate (R_h) will now be recommended, based on the anti-jam performance analysis of Section 2. The allowable jammer-to-signal power ratio J/S changes very little with R_h when the data rate R_b is much lower than R_h (Figs. 3-10), which must be the case on the 50 Kb/s audio/telemetry channels if the 400 Kb/s channels are to be fast-hopped. We therefore begin our recommendations with those channels where the anti-jam performance is sensitive to R_h, namely, the forward link and the video return channel.

Given a bit error probability P_b and an integer k between 2 and 5, the rate 1/2, dual-k convolutional codes offer a coding gain of at least 3 dB in worst-case J/S performance over 2^k-dimensional block orthogonal coding on these 400 Kb/s links, when the hop rate R_h is chosen at the

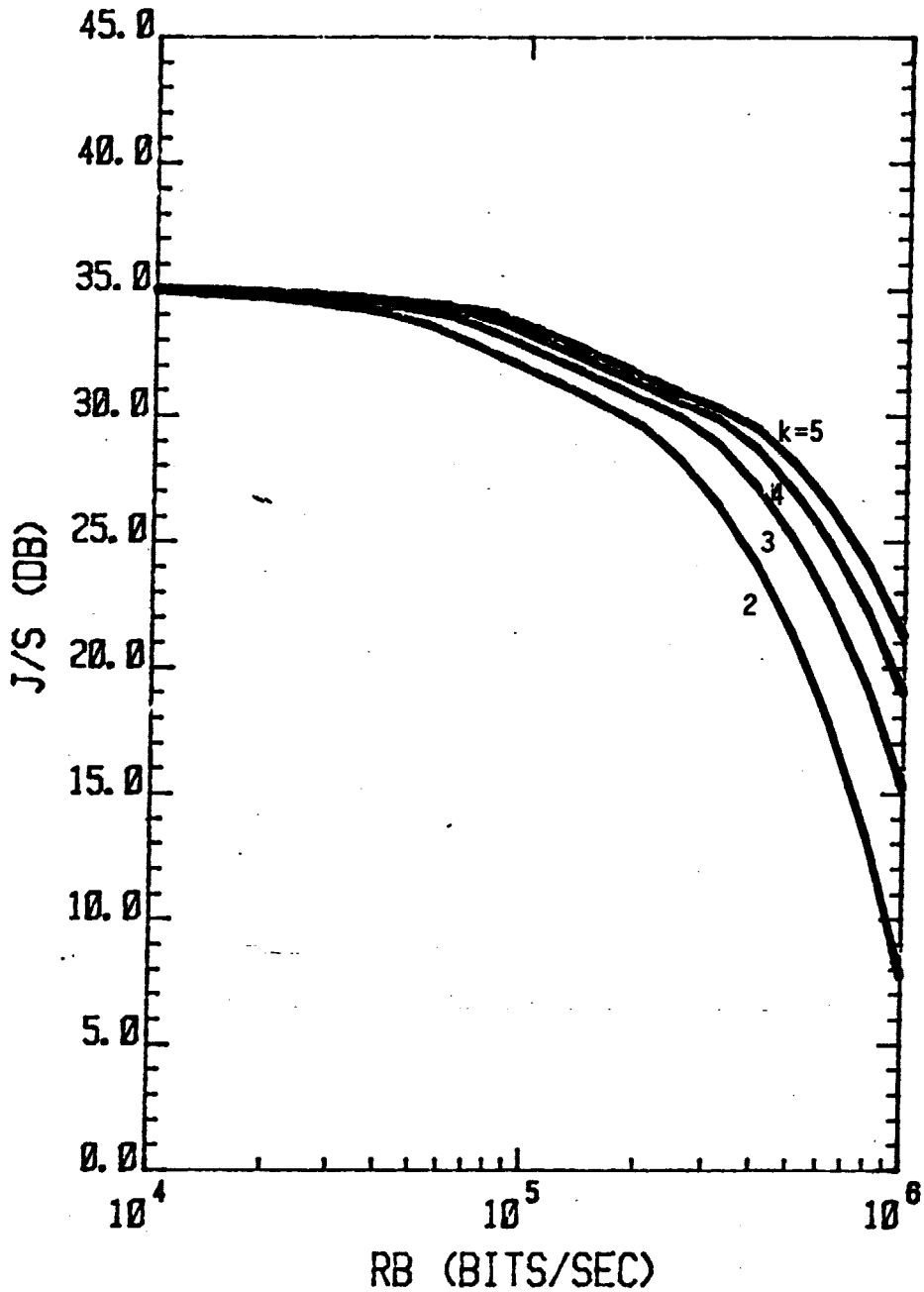

Figure 11. Maximum Allowable Jammer-to-Signal Power Ratio (J/S) in Worst-Case Jamming for Block-Orthogonally Coded 2^k-ary FSK, W = 2 GHz, R_h = 600 kilohops/sec, $P_b = 10^{-3}$.

peak of the dual-k curves (Figs. 3-10). There are dual-k codes that can be decoded more easily than other types of convolutional codes, so a rate 1/2, dual-k code is recommended on the forward link and the video return channel. Although the peak J/S gain of dual-4 over dual-3 codes varies from about 2 to 1 dB (Figs. 5, 6, 9, and 10), the peak gain of dual-5 over dual-4 ranges from only 1 to about 0.5 dB. The former gain justifies the cost of doubling the number of filters in the SOC video demodulators and all of the EVA and free-flyer multiple-access demodulators, but the dual-5 incremental gain does not. We therefore recommend a rate 1/2, dual-4 convolutional code for each of the 400 Kb/s channels.

The hop rate R_h that most effectively alleviates worst-case jamming on these channels is the one that maximizes the worst-case multitone J/S (Figs. 9 and 10), since the J/S values for partial band jamming (Figs. 5 and 6, respectively) are higher, even at the peaks of the multitone curves. The peak occurs when R_h is near 512 kilohops/sec (Khops/s) for a bit error probability P_b of 10^{-3} (Fig. 10); if $P_b = 10^{-5}$, R_h should be increased to about 600 Khops/s (Fig. 9).

When these hop rates are applied to the 50 Kb/s video return channels, the coding gain in allowable J/S of the dual-k codes over the 2^k-dimensional block orthogonal codes is no more than 1 dB for $P_b = 10^{-3}$ (Figs. 12 and 13), and is less than 2 dB if $P_b = 10^{-5}$ (Figs. 14 and 15). Even for the practical dual-k codes, the additional cost of dual-k code implementation over block orthogonal coding cannot be offset by gains so small. The number k of bits/M-ary symbol also makes little difference (Figs. 12-15) in J/S performance, so we recommend just 2 bits/symbol, because this requires only 4 filters in each SOC

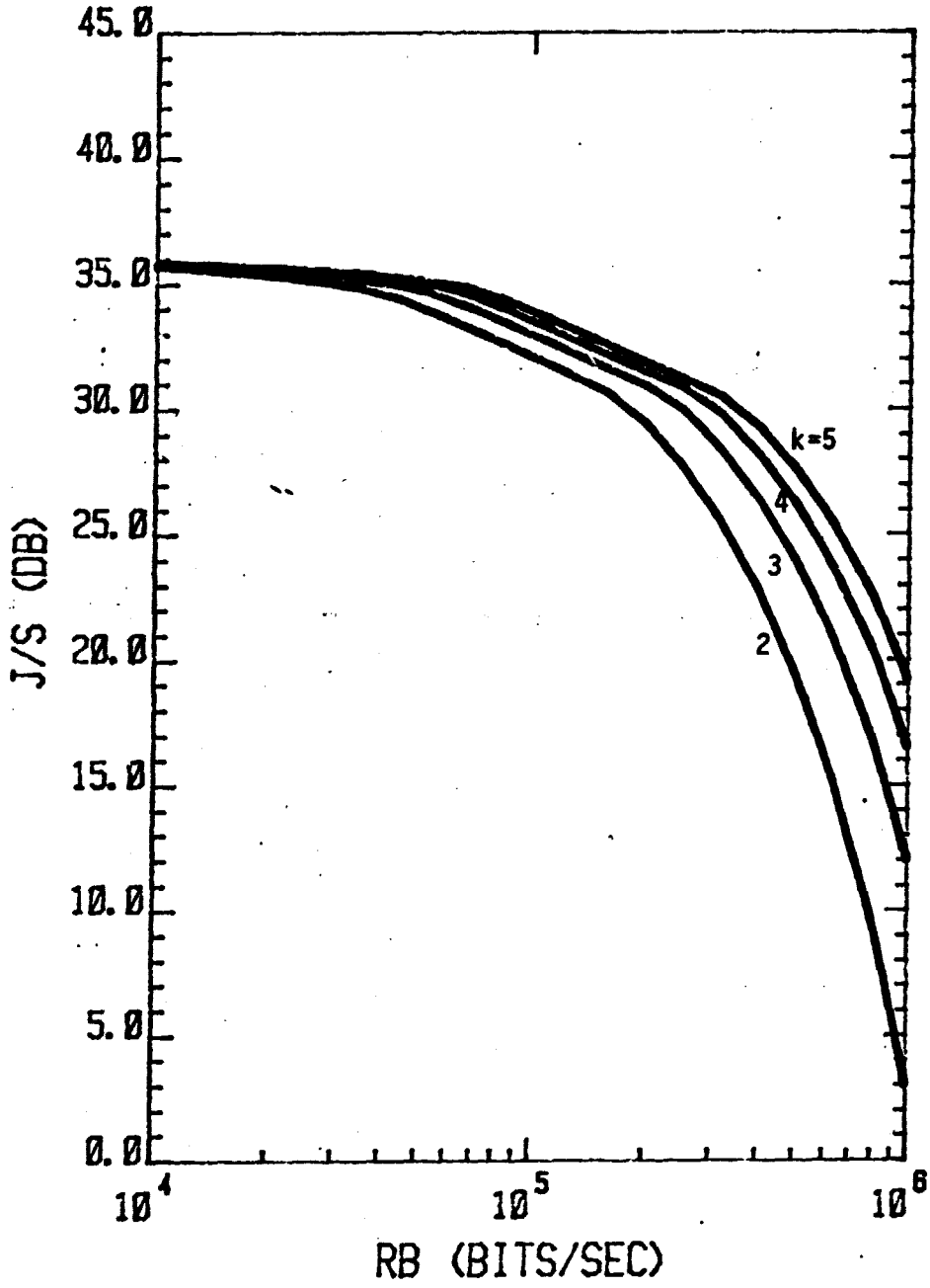

Figure 12. Maximum Allowable Jammer-to-Signal Power Ratio (J/S) in Worst-Case Jamming for Block-Orthogonally Coded 2^k-ary FSK, W = 2 GHz, R_h = 500 kilohops/sec, $P_b = 10^{-3}$.

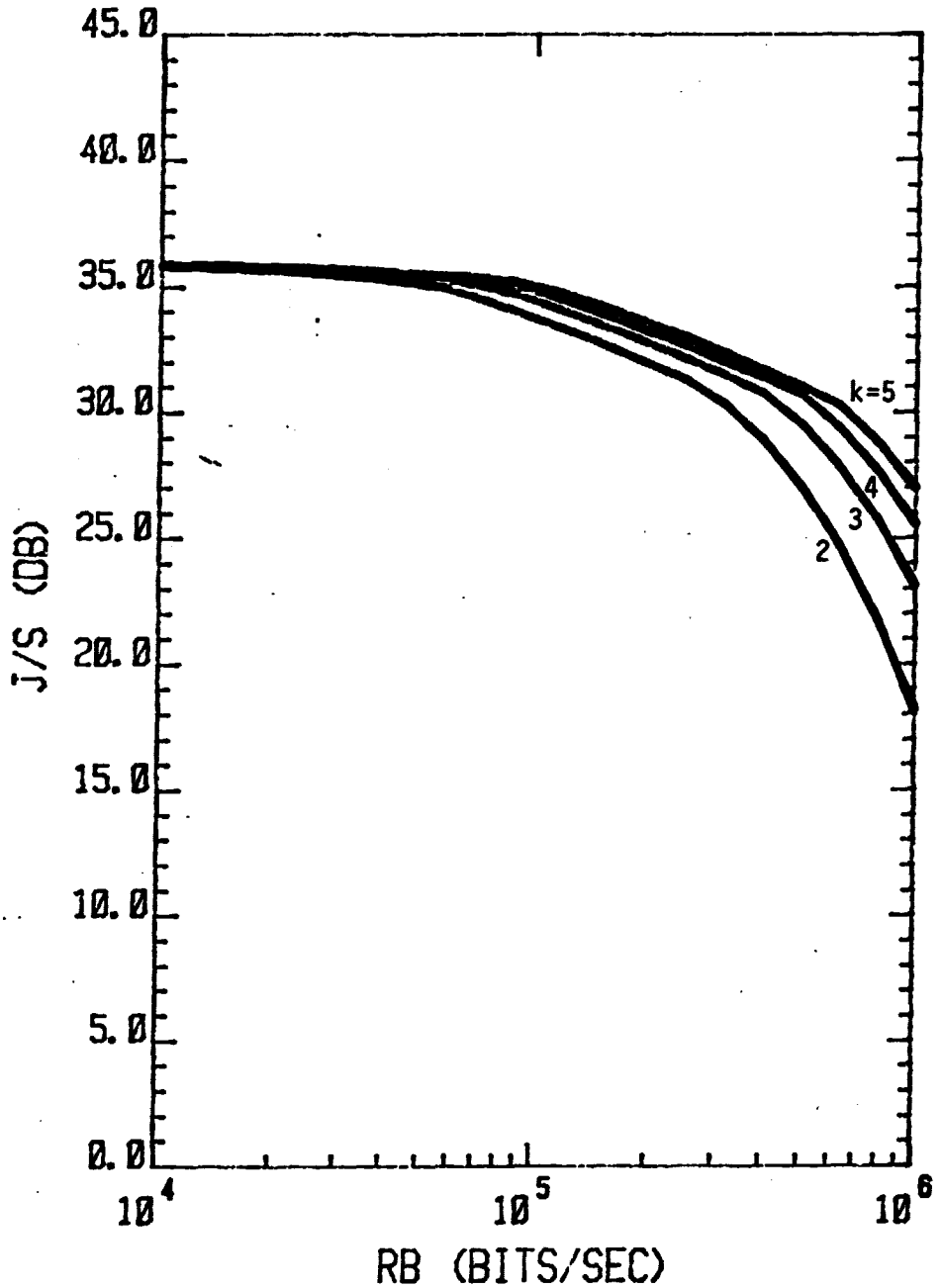

Figure 13. Maximum Allowable J/S in Worst-Case Jamming for Rate 1/2, Dual-k Coded 2^k-ary FSK, W = 2 GHz, R_h = 500 kilohops/sec, $P_b = 10^{-3}$.

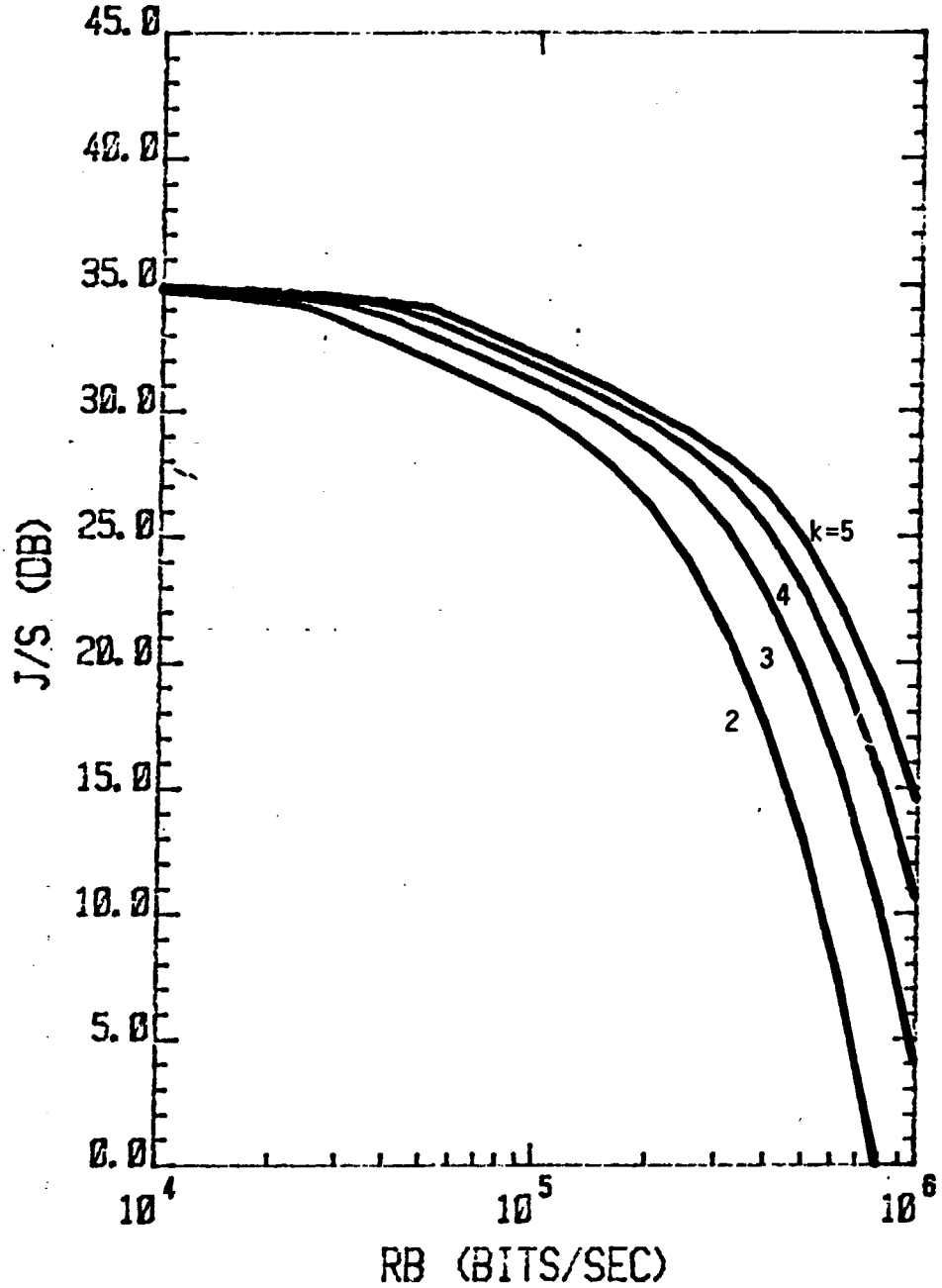

Figure 14. Maximum Allowable J/S in Worst-Case Jamming for Block-Orthogonally Coded 2^k-ary FSK, W = 2 GHz, R_h = 600 kilohops/sec, $P_b = 10^{-5}$.

ORIGINAL PAGE IS
OF POOR QUALITY

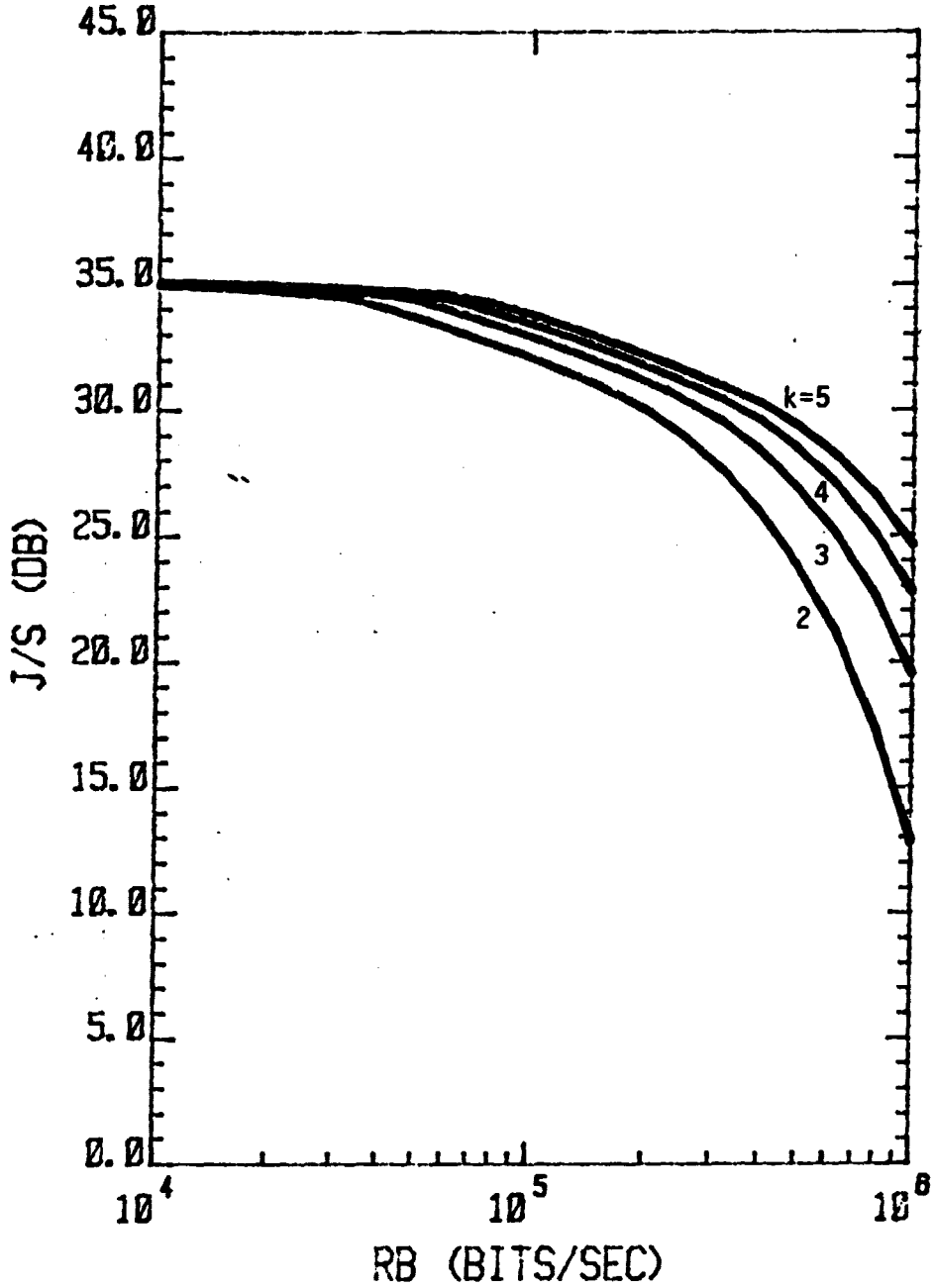

Figure 15. Maximum Allowable J/S in Worst-Case Jamming for Rate 1/2, Dual-k Coded 2^k-ary FSK, W = 2 GHz, R_h = 600 kilohops/sec, $P_b = 10^{-5}$.

audio/telemetry demodulator. Hence 4-ary block orthogonal coding should be used on the audio/telemetry return channel. The channel coding and hop rate recommendations for the forward and return links are summarized in Table I, along with the allowable values of J/S that these recommendations yield (Figs. 9, 10, 12, and 14).

Table I. Recommended Codes and Hop Rates.

LINK	PROPOSED DATE RATE (Kb/s)	REQUIRED BIT EPROR PROB.	RECOMMENDED CODE	RECOMMENDED HOP RATE (Khops/s)	MAXIMUM J/S (dB)
FORWARD	400	10^{-3}	Dual-4, Rate 1/2	512	32
		10^{-5}		600	30
VIDEO RETURN	400	10^{-3}	Dual-4, Rate 1/2	512	32
		10^{-5}		600	30
AUDIO/ TELEMETRY RETURN	50	10^{-3}	4-ary FSK	512	34
		10^{-5}		600	32

REFERENCES

1. Tu, K., "SOC Communications and Tracking," Presented at Lyndon B. Johnson Space Center, Houston, TX, Sept. 1981.

2. Viterbi, A. J., and Jacobs, I. M., "Advances in Coding and Modulation for Noncoherent Channels Affected by Fading, Partial Band, and Multiple-Access Interference," Advances in Communication Systems, Vol. 4, Academic Press, New York, 1975, pp. 279-308.

3. Trumpis, B. D., "On the Optimum Detection of Fast Frequency Hopped MFSK Signals in Worst Case Partial Band Jamming," Presented in Hacienda Hotel Dining Room, 525 N. Sepulveda Blvd., El Segundo, CA, April 1981.

4. Lindsey, W. C., "Error Probabilities for Rician Fading Multichannel Reception of Binary and N-ary Signals," IEEE Transactions on Information Theory, Vol. IT-10, No. 4, Oct. 1964, pp. 339-351.

5. White, M. A., "Maximum Jammer-to-Signal Power Ratio for Fast Frequency-Hopped M-ary FSK in Worst-Case Partial Band Noise Jamming," LinCom Corporation Internal Memo, May 1982.

6. Abramowitz, M., and Stegun, I., (editors), Handbook of Mathematical Functions, National Bureau of Standards Applied Mathematics Series, No. 55, 1972, Chapters 3 and 22.

7. White, M. A., "Performance Comparison of Rate 1/2, Dual-k Convolutional Codes with M-Dimensional Block Orthogonal Codes for Fast Frequency-Hopped M-ary FSK Signals in Worst-Case Jamming," LinCom Corporation Internal Memo, May 1982.

8. Lindsey, W. C., Biederman, L., and Braun, W. R., "Investigation of AJ/LPE Signal Processing Techniques for Mobile Users at EHF," LinCom Corporation Final Report TR-0781-2379, July 15, 1980, SECRFT.

ATTACHMENT 3

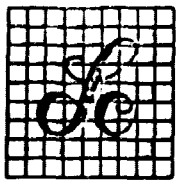

LinCom Corporation

INTEROFFICE MEMORANDUM
TM-0582-1080a

Date: May 11, 1982

From: Mike White

To: L. Biederman

Subject: Maximum Jammer-to-Signal Power Ratio for Fast Frequency-Hopped M-ary FSK in Worst-Case Partial Band Noise Jamming

---

The received jammer-to-signal power ratio (J/S) depends on the fraction ρ ($0 < \rho \leq 1$) of the frequency-hopping bandwidth W that is jammed. The worst-case jammer increases ρ with the hop rate R_h, until $\rho = 1$ and the jamming is broadband. Trumpis [1] has presented the bit error probability P_b as a funtion of W, M, R_h, J/S, the data rate R_b, and the number m of hops per M-ary symbol, when ρ is at its worst possible value.

For $\rho < 1$, the exact P_b is [1]

$$P_b = K'(m,M) \left[\frac{JR_h}{SW} \right]^m, \quad \rho < 1 \qquad (1)$$

where

m: number of hops/symbol, or diversity

W: frequency-hopping, or spread, bandwidth

X_0: largest value of bit energy-to-noise density ratio $(S/R_b)/(J/W)$ such that $\rho = 1$

K'(m,M): proportionality constant, depending on m and M.

To clarify the relationship between J/S and m, we approximate K' with an explicit function of the chips/symbol, or diversity, m.

$$K'(m,M) \doteq K''(M)10^{A(M)\cdot m} \qquad (2)$$

where A(M) and K"(M) are unitless constants, which vary only with M. Substituting (2) into (1) gives

$$P_b \doteq K''(M)\left[\frac{10^{A(M)}JR_h}{SW}\right]^m, \quad \rho < 1 \qquad (3)$$

In broadband noise, the exact bit error probability can be inferred from the exact error probability P_{BFSK} for binary frequency-shift keying (BFSK). P_{BFSK} is a function of half the symbol energy-to-noise density ratio z, which is given by

$$z = \frac{kSW}{2JR_b} \qquad (4)$$

where k is the number of bits/M-ary symbol, i.e.,

$$M = 2^k \qquad (5)$$

Lindsey [2] has derived P_{BFSK} as a function of m and z in broadband noise,

$$P_{BFSK} = 2^{-m}e^{-z}\sum_{i=0}^{m-1} 2^{-i}L_i^{(m-1)}(-z), \quad \rho = 1 \qquad (6)$$

where m must be a positive integer and $L_i^{(m-1)}(-z)$, i = 0,1,2,...,m-1, is the i-th generalized Laguerre polynomial of order (m-1) [3], defined recursively by

$$L_0^{(m-1)}(x) = 1$$

$$L_1^{(m-1)}(x) = -x + m$$

$$L_i^{(m-1)}(x) = \frac{1}{i}(-x+m+2i+2)L_{i-1}^{(m-1)}(x) - \frac{2}{i}(m+i-2)L_{i-2}^{(m-1)}(x),\ i = 2,\ldots,m-1 \tag{7}$$

For MFSK, we assume the M possible FSK chips to be separated by a multiple of R_h, so the signal set is orthogonal. In this case, the bit error probability P_b for MFSK in broadband noise jamming is [4]

$$P_b < \frac{M}{2} P_{BFSK},\quad \rho = 1 \tag{8}$$

Although (8) contains an inequality, there is no significant difference between P_b and $\frac{M}{2} P_{BFSK}$ when $P_b \leq 10^{-3}$. Substituting (5) and (6) into (8) yields

$$P_b < 2^{k-1-m} e^{-z} \sum_{i=0}^{m-1} 2^{-i} L_i^{(m-1)}(-z),\ \rho = 1 \tag{9}$$

Expressions (3) and (9) for P_b will now be used to determine a maximum jammer-to-signal power ratio (J/S) for a specified bit error probability performance P_b^*. Since P_b^* is a maximum, the actual P_b must satisfy

$$P_b < P_b^* \tag{10}$$

Assuming P_b is given exactly by (3) and (9),

$$P_b^* > \begin{cases} K''(M) \left[\dfrac{10^{A(M)_{JR_h}}}{SW}\right]^m, & \rho < 1 \\ 2^{k-1-m_e-z} \sum_{i=0}^{m-1} 2^{-i} L_i^{(m-1)}(-z), & \rho = 1 \end{cases} \tag{11}$$

Since both expressions on the right hand side of (11) are increasing functions of J/S for $m \geq 1$, the maximum J/S is the one that yields the equality in (11). Solving (4) and (11) for this maximum J/S gives

$$J/S = \begin{cases} \dfrac{W}{10^{A(M)_{R_h}}} \left[\dfrac{P_b^*}{K''(M)}\right]^{1/m}, & \rho < 1 \\ \dfrac{Wk}{2R_b z^*}, & \rho = 1 \end{cases} \tag{12}$$

where z^* is the unique value of z that produces equality in (11).

REFERENCES

[1] Trumpis, B. D., "On the Optimum Detection of Fast Frequency Hopped MFSK Signals in Worst Case Partial Band Jamming," presented April 1981.

[2] Lindsey, W. C., "Error Probabilities for Rician Fading Multichannel Reception of Binary and N-ary Signals," IEEE Transactions on Information Theory, Vol. IT-10, No. 4, Oct. 1964, pp.339-351.

[3] Abramowitz, M., and Stegun, I., (editors), Handbook of Mathematical Functions, National Bureau of Standards Applied Mathematics Series, No. 55, 1972, Chapters 3 and 22.

[4] Wozencraft, J. M., and Jacobs, I. M., Principles of Communication Engineering, Wiley & Sons, New York, 1965, p. 258.

ATTACHMENT 4

LinCom Corporation

INTEROFFICE MEMORANDUM
TM-0582-1080b
Date: May 11, 1982

From: Mike White

To: Leon Biederman

Subject: Performance Comparison of Rate 1/2, Dual-k Convolutional Codes with M-Dimensional Block Orthogonal Codes for Fast Frequency-Hopped M-ary FSK Signals in Worst-Case Jamming

Rate 1/2, dual-k convolutional codes usually offer a performance improvement over M-dimensional block orthogonal codes in worst-case jamming. This improvement depends largely on m, the diversity or number of frequency hops/encoder input, when the codewords are M-ary frequency-shift keyed (MFSK) and fast frequency-hopped. The coding gain G(m) of dual-k coding over block orthogonal coding can be expressed as

$$G(m) \equiv \frac{(J/S)_{\text{dual-k}}}{(J/S)_{\text{block}}} \qquad (1)$$

where $(J/S)_{\text{dual-k}}$ and $(J/S)_{\text{block}}$ are the maximum values of the received jammer-to-signal power ratio (J/S) for rate 1/2, dual-k coding and M-dimensional block orthogonal coding, respectively.

$(J/S)_{\text{dual-k}}$ and $(J/S)_{\text{block}}$ are the largest possible values of J/S that yield a decoded bit error probability P_b below a specified maximum P_b^*.

$$P_b < P_b^* \qquad (2)$$

The frequency distribution of the power J, although fixed for both types of coding, is the one that degrades performance the most, i.e., the worst-case distribution. In addition to P_b^*, $(J/S)_{block}$ and $(J/S)_{dual\text{-}k}$ are functions of the number k of bits in each encoder input, the data rate R_b, the frequency hop rate or chip rate R_h, the total frequency bandwidth W available for hopping, and the type of jamming (noise or CW).

The coding gain G(m) in a given jammed channel is determined by the difference between the rate 1/2, dual-k codes and the M-dimensional block orthogonal codes. For M-dimensional block orthogonal coding, each encoder input consists of k bits, which are encoded into a different orthogonal M-bit, nonzero codeword, where

$$M = 2^k \tag{3}$$

Rate 1/2, dual-k encoders map k-bit inputs into two distinct k-bit, or 2^k-ary, outputs[1] (Figure 1). Although the codeword lengths produced by the two types of coding are different, there are M different codewords in both cases, from (3). Assuming (a) each k-bit input is equally probable, (b) amplitude gains are the same at all signaling frequencies, and (c) R_b, R_h, W, and the worst-case jamming are fixed, the probability P_c that a particular incorrect codeword has as large a chip output at the receiver as the correct codeword does, is the same for M-dimensional block orthogonal coding as it is for rate 1/2, dual-k convolutional coding.

Since P_c is more directly related to J/S than the bit error probability P_b, we derive P_c in terms of J/S before analyzing P_b. Although the channel code does not affect the J/S that can be tolerated in maintaining P_c, the type of jamming must be considered. We assume

that each received chip envelope is clipped at the received signal power S, so the worst-case multitone jammer presumably sends J/S tones, each of received power S. Neglecting signal phase jamming, $(P_c)_{tone}$, the P_c in this CW jamming environment, is the probability that a jammer tone hits a given hop of a particular untransmitted codeword.

$$(P_c)_{tone} = \frac{\#\text{ of jamming tones}}{\#\text{ of hopping tones}} = \frac{J/S}{W/R_h} \qquad (4)$$

$(P_c)_{noise}$, the P_c in partial band noise jamming, has nearly the same value as $(P_c)_{tone}$. The partial band noise jammer jams a fraction ρ ($0 < \rho \leq 1$) of the hopping band W at a constant power level.[1] The worst-case ρ increases with R_h until it reaches 1, where the jamming is actually broadband. Regardless of ρ however,[1]

$$(P_c)_{noise} < 4e^{-1} \frac{J/W}{S/R_h} \qquad (5)$$

Although (5) is an inequality, it asymptotically approaches equality for the region of diversity m where the worst-case $\rho < 1$. Since this region is the one where (a) $(P_c)_{noise}$ is most sensitive to m and (b) most design decisions are made, we infer from (4) and (5) that

$$P_c \doteq K \frac{J/W}{S/R_h} \qquad (6)$$

where K is a unitless constant that depends only on the form of the jamming, either multiple tones or partial band noise. In particular, the probability P_{cd} that a transmitted rate 1/2, dual-k codeword will have a smaller received chip envelope during a given hop than another given dual-k codeword does, is

$$P_{cd} \doteq K \frac{R_h}{W} (J/S)_{dual\text{-}k} \tag{7}$$

For M-dimensional block orthogonal coding, P_c is denoted by P_{cb}, where

$$P_{cb} \doteq K \frac{R_h}{W} (J/S)_{block} \tag{8}$$

For the same hopping band W, hop rate R_h, and jamming environment for these two types of coding, (7) and (8) can be substituted into (1) to give

$$\frac{(J/S)_{dual\text{-}k}}{(J/S)_{block}} \doteq \frac{P_{cd}}{P_{cb}} \tag{9}$$

The coding gain (9) can be expressed in terms of several different error probabilities. We now present these probabilities sequentially to show the relationship between P_c and the bit error probability P_b. Assuming that each of the m chips of each encoder input are optimally combined, all m chip outputs of an untransmitted codeword must be as large as those of the transmitted codeword, before the incorrect codeword can be chosen by the decoder. The probability P_E that this incorrect codeword will be decoded, is therefore

$$P_E < (P_c)^m \tag{10}$$

where m, the diversity, is the number of hops (chips)/encoder input.

For the M-dimensional block orthogonal codes, a union bound on the probability P_{block} of <u>any</u> decoding error is[2]

$$P_{block} < (2^k-1)P_E \tag{11}$$

where k is the number of bits in each encoder input. P_{block}, in turn, is proportional to the bit error probability P_{bb} for the block orthogonal codes.[3]

$$P_{bb} = \frac{2^{k-1}}{2^k-1} P_{block} \tag{12}$$

From (10), (11), and (12),

$$P_{bb} < 2^{k-1}P_{cb}^m \tag{13}$$

We can now compare this performance to the bit error probability P_{bd} for the rate 1/2, dual-k codes which is[4]

$$P_{bd} < \frac{2^{k-1}P_{cd}^{2m}}{[1-P_{cd}^{m-n}-P_{cd}^{n}-(2^k-3)P_{cd}^{m}]^2} \tag{14}$$

where P_{cd} atisfies (7) and n is the number of times that one of the two encoded 2^k-ary symbols is chipped (Fig. 1). The right hand side of (14) is minimized when

$$n = m/2 \tag{15}$$

Although this is impractical when m is odd, little accuracy is sacrificed and much algebraic simplicity is gained by assuming (15) to hold for all m. With this assumption, (14) becomes

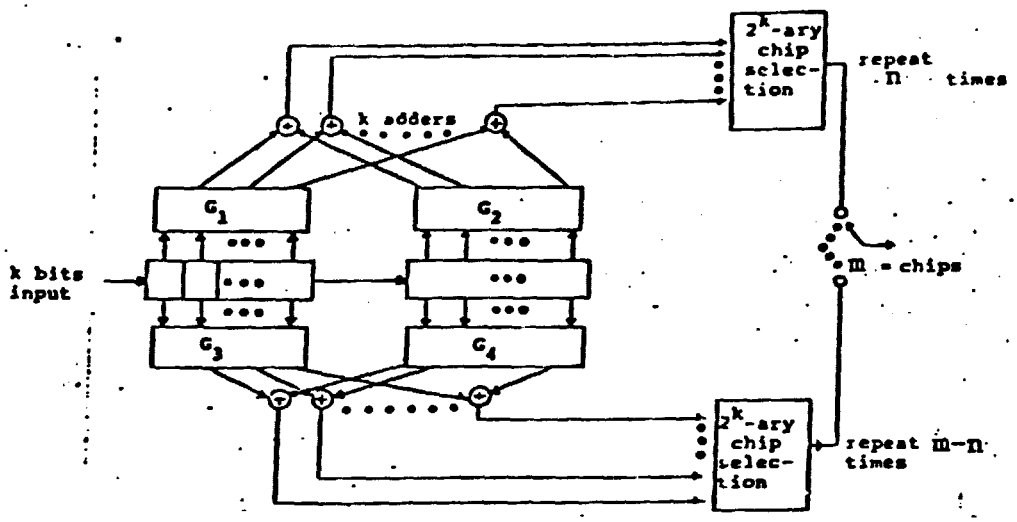

Figure 1. Rate 1/2 Dual-k Encoder.

$$P_b < \frac{2^{k-1}p_{cd}^{2m}}{[1-2p_{cd}^{m/2}-(2^k-3)p_{cd}^m]^2} \tag{16}$$

Assuming that both P_{bb} and P_{bd} must be no larger than the specified maximum bit error probability P_b^*,

$$\begin{aligned} P_{bb} &< P_b^* \\ P_{bd} &< P_b^* \end{aligned} \tag{17}$$

we can now express P_{cb} and P_{cd}, hence $(J/S)_{block}$ and $(J/S)_{dual\text{-}k}$, in terms of this specified performance. (17) will be satisfied when

$$\begin{aligned} 2^{k-1}p_{cb}^m &< P_b^* \\ \frac{2^{k-2}p_{cd}^{2m}}{[1-2p_{cd}^{m/2}-(2^k-3)p_{cd}^m]^2} &< P_b^* \end{aligned} \tag{18}$$

from (13) and (16). The maximum values $(J/S)_{dual\text{-}k}$ and $(J/S)_{block}$ arise when there is equality in (18). Therefore the coding gain G(m) of rate 1/2, dual-k convolutional codes over M-dimensional block orthogonal codes is

$$G(m) \doteq P_{cd}(2^{k-1}/P_b^*)^{1/m} \tag{19}$$

from (1), (9), and (18), where P_{cd} is given implicitly by the lower equality in (18).

It is evident from this lower equality that G(m) is greater than 1 when

$$1 < 2[1-2p_{cd}^{m/2} - (2^k-3)p_{cd}^m]^2 \tag{20}$$

Solving (20) for $P_{cd}^{m/2}$ by the quadratic formula, we have

$$P_{cd}^{m/2} < \frac{\sqrt{2^k(1-1/\sqrt{2})-2+3/\sqrt{2}}-1}{2^k-3} \qquad (21)$$

When (21) is true for m=1, as it is for most coded communication links, the coding gain G(m) of the dual-k codes is always greater than 1, but it decreases toward 1 as the diversity m increases.

REFERENCES

1. Viterbi, A. J., and Jacobs, I. M., "Advances in Coding and Modulation for Noncoherent Channels Affected by Fading, Partial Band, and Multiple-Access Interference," Advances in Communication Systems, Vol. 4, Academic Press, New York, 1975, pp. 279-308.

2. Wozencraft, J. M., and Jacobs, I. M., Principles of Communication Engineering, Wiley & Sons, New York, 1965, pp. 264-265.

3. Viterbi, A. J., and Omura, J. K., Principles of Digital Communication and Coding, McGraw-Hill, 1979, p. 100.

4. Lindsey, W. C., Biederman, L., and Braun, W. R., "Investigation of AJ/LPE Signal Processing Techniques for Mobile Users at EHF," LinCom Final Report TR-0781-2379, Pasadena, CA, July 15, 1980, SECRET.